

1 Title: Characterization of human lightness discrimination thresholds for independent spectral variations

2 Authors: Devin Reynolds, Vijay Singh.

3 Department of Physics, North Carolina Agricultural and Technical State University, Greensboro, NC,  
4 USA.

5

6 **ABSTRACT:** The lightness of an object is an intrinsic property that depends on its surface reflectance  
7 spectrum. The visual system estimates an object's lightness from the light reflected off its surface. The  
8 light reflected also depends on object extrinsic properties of the scene. For stable perception, the visual  
9 system needs to discount variations due to extrinsic properties. We characterize this perceptual stability  
10 for variation in two spectral properties of the scene: the reflectance spectra of background objects and the  
11 intensity of light sources. We use a two-alternative forced-choice task to measure human observers'  
12 thresholds of discriminating computer-generated images of 3D scenes based on the lightness of a  
13 spherical target object in the scene. We measured how the discrimination thresholds changed as we varied  
14 the reflectance spectra of the objects and the intensity of the light sources in the scene, both individually  
15 and simultaneously. For small amounts of extrinsic variations, the thresholds of discrimination remained  
16 constant indicating that the thresholds were dominated by observers' intrinsic representation of lightness.  
17 As extrinsic variation increased, it started affecting observers' lightness judgment and the thresholds  
18 increased. We estimated that the effects of extrinsic variations were comparable to observers' intrinsic  
19 variation in the representation of object lightness. Moreover, for simultaneous variation of these spectral  
20 properties, the increase in threshold square compared to no variation condition was a linear sum of the  
21 corresponding increase in threshold squares for the individual properties, indicating that the variation  
22 from these independent sources combines linearly.

23 **KEYWORDS:** Lightness, Human Psychophysics, Color Vision

24 **PRECIS:** We measure human lightness discrimination thresholds as a function of the amount of variation  
25 in object-extrinsic spectral properties of visual scenes. We show that the visual system largely  
26 compensates for such variations and that the effect of variation in independent properties combines  
27 linearly.

28 **INTRODUCTION**  
29 Our visual system provides perceptual representation of distal properties of objects based on the proximal  
30 stimuli captured by the eyes. While object properties are intrinsic to the object (its color, shape, etc.), the  
31 proximal stimuli also depend on the properties of the scene in which the object lies (such as background  
32 objects in the scene, illumination, etc.) as well as the position and pose of the observer. The task of the  
33 visual system is to provide stable correlates of object intrinsic properties under variability of the proximal  
34 signal due to object extrinsic scene properties. This work quantifies the extent to which the visual system  
35 provides such stability for the representation of the reflectance of an object under variation in spectral  
36 properties of the scene, specifically, variation in the spectra of the background objects and the intensity of  
37 light sources in the scene.

38 The perceptual correlate of the diffuse spectral reflectance of an object is its perceived color. For  
39 achromatic objects, the analogous perceptual quantity is object lightness. The human visual system is  
40 known to provide a relatively stable representation of the color/lightness of an object despite variability in  
41 the proximal signal due to changes in the light source, the surface reflectance of objects in the scene, and  
42 the geometry and other properties of the scene (Foster, 2011; Brainard & Radonjic, 2004). The degree to  
43 which such stability can be achieved is termed as color/lightness constancy (Adelson, 2000; Gilchrist,  
44 2006). Human color/lightness constancy has been measured using appearance-based approaches and  
45 discrimination-based approaches (Olkonen & Ekroll, 2016). Appearance based approaches involve tasks  
46 in which the observer makes judgement about the appearance of stimuli. This approach includes methods  
47 such as color matching, color naming, scaling, and nulling (Foster, 2003). In color matching, observers  
48 adjust a test stimulus to match a standard stimulus. Color matching experiments show varying degrees of  
49 constancy with constancy measured between 15%-90% under conditions such as changes of illumination  
50 (Arend & Goldstein, 1987; Arend & Spehar, 1993), reflectance (Arend & Spehar, 1993; Patel,  
51 Munasinghe, & Murray, 2018), illumination gradients (Arend & Goldstein, 1990; Brainard, Brunt, &  
52 Speigle, 1997), and illumination and simulated reflectance (Rutherford & Brainard, 2002). Color naming  
53 is a more direct and arguably natural method to measure color constancy where observers are asked to  
54 categorize stimuli based on their hue, saturation, and lightness (Troost & De Weert, 1991). This method  
55 has been used with real (Uchikawa, Uchikawa, & Boynton, 1989; Olkkonen, Witzel, Hansen, &  
56 Gegenfurtner, 2010) and simulated stimuli (Olkonen, Hansen, & Gegenfurtner, 2009) to measure  
57 constancy. Color naming methods have the limitation that there are vast number of possible discernible  
58 colors (Linhares, Pinto, & Nascimento, 2008), but there is a limit of the gamut that can be displayed.  
59 Typically, observers are asked to name from a small set of colors (Speigle & Brainard, 1996; Smithson &  
60 Zaidi, 2004; Hansen, Walter, & Gegenfurtner, 2007) which might provide an overestimate of the  
61 measured constancy. In color scaling methods, observers view a stimulus and provide a rating on a scale  
62 for a set of colors, thus allowing for a finer level of comparison for measuring constancy (Luo, et al.,  
63 1991; Schultz, Doerschner, & Maloney, 2006). Scaling methods can also be used to measure changes in  
64 stimuli, where observers provide a rating of the change between stimuli (Ennis & Doerschner, 2019).  
65 Nulling or achromatic adjustment methods involve changing a test stimulus such that it appears  
66 achromatic (Arend, 1993; Brainard, 1998; Delahunt & Brainard, 2004). This method has the limitation  
67 that it provides data only for achromatic/gray stimuli and additional assumptions about the observers'  
68 criterion needs to be made for color appearances (Speigle & Brainard, 1996).

69 Discrimination-based approaches provide an objective method to measure color constancy (Bramwell &  
70 Hurlbert, 1996; Reeves, Amano, & Foster, 2008). In these experiments, observers discriminate stimuli as  
71 to whether they are the same or different from each other. The stimuli are varied in some relevant  
72 parameter space to measure the threshold for discriminating changes in the parameter (Craven & Foster,  
73 1992; Pearce, Crichton, Mackiewicz, Finlayson, & Hurlbert, 2014; Aston, Radonjic, Brainard, &  
74 Hurlbert, 2019). Recently, Singh et. al (Singh, Burge, & Brainard, 2022) developed an equivalent noise  
75 paradigm that relates thresholds of discrimination to the variability in observers' intrinsic representation  
76 of object properties (e.g., its lightness) and the variability due to object extrinsic properties of the scene.

77 They measured human lightness discrimination thresholds as a function of the amount of variability in the  
78 spectra of background objects in a scene. They related the discrimination thresholds to the variance in  
79 observers' internal perceptual representation of lightness and the variance in the spectrally induced  
80 extrinsic variability. A comparison of the strength of intrinsic and extrinsic variability provided a measure  
81 of the degree of constancy in the object intrinsic property due to the variability in object extrinsic  
82 property.

83 This equivalent noise paradigm can also be used to compare the effect of different sources of variabilities.  
84 The variance of multiple extrinsic properties can be characterized relative to the variance of the intrinsic  
85 variability. These in turn can be compared to each other to measure their relative effects. It can also be  
86 used to characterize how the effect of multiple sources of variability combine when presented  
87 simultaneously.

88 In this work, we use this paradigm to compare the variation in two spectral properties of the scene to  
89 human observers' representation of lightness. The spectral variations we study are: the surface reflectance  
90 of the background objects in the scene and the intensity of the light sources in the scene. We measure  
91 human observers' threshold of discriminating two images based on the lightness of an achromatic target  
92 object in the images. We measure how these discrimination thresholds change as we increase the  
93 variability in the reflectance spectra of the background objects and the intensity of the light sources. We  
94 measure discrimination thresholds for individual and simultaneous variation of these properties. We use  
95 the equivalent noise paradigm to relate the thresholds to the variance of observers' intrinsic noise and the  
96 extrinsic variability. These variances allow one to compare the relative effect of these spectral variations.  
97 A comparison of variance of individual and simultaneous variation condition can provide information  
98 about the combination rules of multiple sources of variation.

99 We show that as the variability in the extrinsic sources increases, initially for small amount of variation,  
100 the thresholds remain constant. In this region, the thresholds are determined primarily by the variation in  
101 observers' internal representation of lightness. As the variability increases further, the discrimination  
102 thresholds increase. The increase in thresholds can be accounted for by a model based on signal detection  
103 theory. This model shows that the effect of extrinsic variation is within a factor of two compared to the  
104 variability in the intrinsic representation of lightness. This confirms that the visual system provides a  
105 large degree of lightness constancy under object extrinsic scene variation. By comparing the increase in  
106 thresholds of the individual and simultaneous variation condition from the no extrinsic variation  
107 condition, we show that the effects of individual sources combine linearly under simultaneous variation.

108 The paper is organized as follows. Section 2, Experimental Methods, provides the details of the  
109 experimental methods, stimuli used, and model fitting. Section 3, Results, provides the results of three  
110 experiments: variation in background reflectance spectra, variation in light source intensity, and  
111 simultaneous variation in these two properties. Section 4, Discussion, provides a summary of the results  
112 and remarks.

## 113 **2 EXPERIMENTAL METHODS**

### 114 **Overview**

115 We followed the methodology published previously in (Singh, Burge, & Brainard, 2022). In this previous  
116 work, human lightness discrimination thresholds were measured under variability of the reflectance  
117 spectra of background objects in the scene. The work presented here follows the same experimental  
118 methods, except that the stimuli used in the experiments are different. This section provides an overview  
119 of the methods, focusing on the differences from the previous work. We refer the reader to the previous  
120 work for details.

121 Similar to the previous work, we used a two-alternative forced-choice (2AFC) procedure to measure  
122 thresholds (Figure 1). On each trial of the experiment, observers viewed pairs of computer-generated 3D  
123 scenes displayed on a color calibrated monitor. These pairs consisted of a standard image and a  
124 comparison image. The images were presented sequentially for 250ms, with a 250ms inter-stimulus  
125 interval between them. Both images contained a centrally located achromatic sphere as the target object.  
126 Observers were required to indicate the image on which the target object was lighter. Between trials, we  
127 manipulated the luminous reflectance factor (LRF) of the target object in the comparison image. The LRF  
128 is defined as the ratio of the luminance of a surface under a reference illuminant and the luminance of the  
129 reference illuminant itself (American Society for Testing and Materials, 2017). The reference illuminant  
130 was chosen as CIE D65 reference illuminant. The order of the standard and the comparison image was  
131 chosen in a pseudorandom order. We plotted the psychometric functions of the observers by collecting  
132 data on the proportion of times the observer chose the comparison image to be lighter (see Figure 2 for an  
133 example). To estimate observers' discrimination threshold, we fit the proportion comparison chosen data  
134 with a cumulative normal function. We defined the threshold as the difference between the LRF of the  
135 target object for which the cumulative normal fit was equal to 0.76 and 0.50. This corresponds to a d-  
136 prime of 1 in a two-interval task.

137 We measured the effect of variation in two types of object-extrinsic scene properties on human lightness  
138 discrimination thresholds: variation in the reflectance spectra of the background objects in the scene and  
139 variation in the intensity of the light sources in the scene. We performed three experiments. These  
140 experiments were preregistered (see below Preregistration).

141 (1) Background reflectance spectra variation (preregistered as Experiment 6): In this experiment, we  
142 measured human lightness discrimination thresholds as a function of the amount of variation in the  
143 background objects while the spectra of the light sources were kept fixed.

144 (2) Light source intensity variation (preregistered as Experiment 7): In this experiment, we measured  
145 lightness discrimination thresholds as a function of the amount of variation in the intensity of the light  
146 sources while the background was fixed.

147 (3) Simultaneous variation (preregistered as Experiment 8): In this experiment, we measured lightness  
148 discrimination thresholds as both the background object reflectance spectra and the light source intensity  
149 varied simultaneously.

150 To study the effect of variation in surface reflectance of background objects we generated samples of  
151 surface reflectance spectra from a multivariate normal distribution. The distribution was a statistical  
152 model of database of natural surface reflectance measurements. The amount of variation in the surface  
153 reflectance of background objects was varied by changing the size of the covariance matrix of the  
154 multivariate normal distribution. We measured discrimination thresholds for both chromatic and  
155 achromatic variations. In chromatic variation, the reflectance spectra could take any shape and the objects  
156 varied in their luminance and chromaticity. In achromatic variation, the reflectance spectra were  
157 spectrally flat, and the objects were gray.

158 The shape of the spectral power distribution function of the light source was chosen as CIE D65 reference  
159 illuminant. The intensity was varied by multiplying the spectral power distribution function by a scalar  
160 sampled from a log uniform distribution. The amount of variation was controlled by changing the range  
161 of the log uniform distribution.

162 The subsections below provide additional methodological detail.

163 **Preregistration**

164 We preregistered the experiments performed in this work before collecting the data. The preregistration  
165 documents are available at: <https://osf.io/7tgy8/>.<sup>1</sup> The documentation includes information about the  
166 experimental design as well as the procedure to estimate thresholds from the collected data.

167 The experiments were preregistered as Experiment 6 (referred here as Background reflectance spectra  
168 variation), Experiment 7 (referred here as Light source intensity variation), and Experiment 8 (referred  
169 here as Simultaneous variation). Experiment 6 was a replication of previous work (preregistered as  
170 Experiment 3; Singh, Burge, & Brainard, 2022) with additional conditions in which the background  
171 objects were achromatic and varied only in their lightness. While the stimuli were different for the three  
172 experiments (preregistered Experiments 6, 7, and 8), the experimental method to measure lightness  
173 discrimination thresholds were the same.

174 The preregistration documents mentioned that the experiments aimed at characterizing the dependence of  
175 human lightness discrimination thresholds on the amount of variation in the background reflectance and  
176 the intensity of the light source in the scene. The method of estimating discrimination thresholds was  
177 described in the document. We predicted that the thresholds would increase with increase in the amount  
178 of variation. For background variation, we predicted that the thresholds of achromatic variation would be  
179 lower than chromatic variation. We also predicted that the increase in thresholds could be captured by an  
180 equivalent noise model (Singh, Burge, & Brainard, 2022). Additionally, we predicted that the threshold  
181 for simultaneous variation would be higher than the thresholds for individual variations.

## 182 Reflectance and Illumination Spectra

183 We used a statistical model of natural reflectance dataset to generate reflectance spectra of background  
184 objects (Singh, Cottaris, Heasly, Brainard, & Burge, 2018; Singh, Burge, & Brainard, 2022). We  
185 combined two datasets of surface reflectance measurements (Vrhel, Gershon, & Iwan, 1994; Kelly,  
186 Gibson, & Nickerson, 1943). These datasets contain 632 surface reflectance measurements. We mean  
187 centered the dataset by subtracting out the mean surface reflectance over the 632 measurements. Then we  
188 used principal component analysis (PCA) to obtain the projection of the mean centered dataset along the  
189 eigenvectors associated with the six largest eigenvalues. These eigenvalues captured more than 99.5% of  
190 the variance (Singh, Cottaris, Heasly, Brainard, & Burge, 2018). The empirical distribution of the  
191 projection weights thus obtained was approximated with a multivariate normal distribution. To get the  
192 projection weights of random samples of reflectance spectra, pseudorandom samples were generated from  
193 this multivariate normal distribution. Reflectance spectra were constructed by using these projection  
194 weights along with the eigenvectors and adding the mean of the surface reflectance dataset. A physical  
195 realizability condition was imposed on these spectra by ensuring that the reflectance at each wavelength  
196 was between 0 and 1. If a reflectance spectrum did not meet this criterion, it was discarded.

197 To generate achromatic surface reflectance spectra, after generating a physically realizable reflectance  
198 spectrum, its average reflectance over all wavelengths was calculated and it was replaced by a spectrum  
199 which had this average reflectance at all wavelengths.

200 To control the amount of variation in the reflectance spectra, the covariance matrix of the multivariate  
201 normal distribution was multiplied by a covariance scalar ( $\sigma^2$ ). A covariance scalar of 0 indicates that  
202 there is no variation in the reflectance spectra of the background objects. On the other hand, a covariance

---

<sup>1</sup> The preregistration documents relevant to this work are those for Experiments 6, 7 and 8. The site also contains preregistrations for previously reported (Experiment 1, 2 and 3; Singh, Burge, & Brainard, 2022) and unreported (Experiment 4 and 5) work.

203 scalar of 1 corresponds to the range of reflectance variation observed in the combined natural reflectance  
204 datasets.

205 The light source power spectrum was chosen to be CIE D65 reference illuminant. The D65 spectrum was  
206 divided by its mean power over wavelength to obtain its relative spectral shape. The variation in the light  
207 source intensity was introduced by multiplying the normalized D65 spectrum by a random sample  
208 generated from a log-uniform distribution in the range  $[1 - \delta, 1 + \delta]$ , where  $\delta$  determines the range of the  
209 distribution. We chose log-uniform distribution for the multiplication parameter because the spectral  
210 power distribution function of natural daylight spectra varies over three orders of magnitude and their  
211 mean over wavelength can be roughly approximated by a log-uniform distribution (Singh, Cottaris,  
212 Heasly, Brainard, & Burge, 2018). All light sources in a scene were assigned the same power spectrum.

213 The values of the two parameters  $\sigma^2$  and  $\delta$  for the three experiments were as follows:

214 Background object reflectance variation (Experiment 6): In this experiment, we generated images for nine  
215 conditions. Six of these conditions were for chromatic variation at six logarithmically spaced values of the  
216 covariance scalar ( $\sigma^2$ ): [0, 0.01, 0.03, 0.1, 0.3, 1.0] (same as Singh, Burge, & Brainard, 2022). Three  
217 conditions were for achromatic variation at covariance scalar ( $\sigma^2$ ): [0.03, 0.3, 1.0]. The power spectrum  
218 of the light source was the same for all images. The power spectrum multiplication scalar was assigned an  
219 arbitrary value of 5. Figure 3 shows five typical images for the nine conditions.

220 Light source intensity variation (Experiment 7): In this experiment, we generated images for seven  
221 linearly spaced values of the range parameter ( $\delta$ ): [0.00, 0.05, 0.10, 0.15, 0.20, 0.25, 0.30]. The  
222 reflectance spectra of all background objects were the same and were equal to the mean spectrum of the  
223 reflectance database. This corresponds to covariance scalar of 0. Figure 4 shows five typical images for  
224 the seven conditions.

225 Simultaneous variation (Experiment 8): In this experiment we studied six conditions. These were: no  
226 variation ( $\sigma^2 = 0, \delta = 0$ ), chromatic background variation (covariance scalar = 1,  $\delta = 0$ ), achromatic  
227 background variation ( $\sigma^2 = 1, \delta = 0$ ), light source intensity variation ( $\sigma^2 = 0, \delta = 0.3$ ), simultaneous  
228 variation chromatic background ( $\sigma^2 = 1, \delta = 0.3$ ) and simultaneous variation achromatic background ( $\sigma^2$   
229 = 1,  $\delta = 0.3$ ). Figure 5 shows five typical images for these six conditions.

## 230 **Stimulus Design**

231 The images used in this work were generated using the software Virtual World Color Constancy (VWCC)  
232 ([github.com/BrainardLab/VirtualWorldColorConstancy](https://github.com/BrainardLab/VirtualWorldColorConstancy)) described in (Singh, Cottaris, Heasly, Brainard,  
233 & Burge, 2018). The initial step to generate an image involves constructing a 3D model that serves as the  
234 base scene. Then, based on the specific experimental condition, we assign reflectance spectra and spectral  
235 power distribution functions to the objects and light sources within the base scene. All light sources  
236 within a given scene were assigned identical spectral power distribution functions. Subsequently, we  
237 utilize Mitsuba, an physically-realistic open-source rendering system ([mitsuba-renderer.org](http://mitsuba-renderer.org); Jakob, 2010)  
238 to produce a 2D multispectral image of the scene. A 201-pixel by 201-pixel part of the image centered at  
239 the target object was cropped out to display on the monitor. Monitor calibration data was used to convert  
240 the multispectral images to gamma corrected RGB images as described in (Singh, Burge, & Brainard,  
241 2022). Gamma-corrected RGB images were presented on the calibrated monitor during the experiment.  
242 When displayed on the experimental monitor at a distance of 75cm from the observers' head position, the  
243 image was nearly 2° in visual angle with the target nearly 1° in visual angle.

244 For each condition described above, we generated 1100 images, 100 images each at each of the 11  
245 linearly spaced values of the target object LRF in the range [0.35, 0.45]. The standard image target object  
246 LRF was 0.4. The comparison image target object LRF varied in the range [0.35, 0.45]. We generated 100  
247 images at each comparison level to avoid excessive replication of images in the experiment. For the no  
248 variation ( $\sigma^2 = 0.00$ ,  $\delta = 0.00$ ) condition, we generated one image at each target object LRF level, as the  
249 background reflectance and the light source intensity remained fixed in this case. The scene geometry  
250 remained fixed during the experiment and the images did not include secondary reflections.

251 The standard image, when presented on the experimental monitor, had an average luminance of 87.1  
252 cd/m<sup>2</sup> for the condition ( $\sigma^2 = 0.00$ ,  $\delta = 0.00$ ). The average luminance of the target object for the 11 LRF  
253 levels were [120.9, 122.3, 123.8, 125.2, 126.5, 127.9, 129.2, 130.5, 131.9, 133.1, 134.4] cd/m<sup>2</sup>.

254 For the ( $\sigma^2 = 1.00$ ,  $\delta = 0.30$ ) condition, the average luminance of the standard image was 87.8 cd/m<sup>2</sup>. The  
255 average luminance of the target object for the 11 LRF levels were [117.7, 119.4, 119.4, 122.3, 123.7,  
256 123.8, 127.8, 126.9, 127.7, 129.1, 129.0] cd/m<sup>2</sup>.

## 257 **Experimental Structure:**

258 In this study, a trial is defined as the display of a standard and a comparison image on the monitor and the  
259 recording of the observer's response. An interval is defined as the presentation of either the standard  
260 image or the comparison image within a trial. A block consists of recording 330 trials for one condition,  
261 30 trials each at 11 comparison image target LRF levels. A permutation consists of recording one block of  
262 data for each condition in an experiment. We recorded three permutations for each observer in each  
263 experiment. Each permutation had a random order of the conditions.

264 The order of the blocks in a permutation, the LRF levels of the comparison image in trials of a block, and  
265 the order of standard and comparison images in a trial was generated pseudorandomly and stored at the  
266 beginning of the experiment for each observer. Before starting a new permutation for an observer, the  
267 data for all blocks (conditions) in a permutation was collected.

268 A session consisted of recording three blocks on a single day. An observer performed no more than one  
269 session on a day. Each block in a session was divided into three sub-blocks of 110 trials. Between these  
270 sub-blocks, the observers took a break of minimum one minute. The observers also took a small break  
271 (nearly two to five minutes) between blocks. The observers were informed that they could stop the  
272 experiment at any time. If the observer terminated a block, the data was not recorded. No observer  
273 terminated a block of the experiment.

274 Each observer first performed a practice session where three blocks of data was recorded for the no  
275 variation ( $\sigma^2 = 0$ ,  $\delta = 0$ ) condition. The observers were excluded from the experiment if their mean  
276 threshold for the last two blocks was higher than 0.03. If the observer passed this criterion, then the rest of  
277 the data was collected over several days.

278 The experimental procedure was explained to each observer at the beginning of the practice session. The  
279 experimenter then obtained the consent for the experiment. Vision tests were performed on the observer  
280 to ensure normal visual acuity and normal color vision. After this, the observer went to the experimental  
281 room where they were familiarized with the experimental set-up by performing a familiarization block of  
282 40 trials. Then the observers were dark adapted by sitting in the dark for about 5 minutes. Then the data  
283 for the three blocks of the practice session was recorded. At the end of the practice session, the observers  
284 were informed if they could continue the experiment.

285 If the observer was continued, their data was collected over several sessions. The data for all six observers  
286 of an experiment was collected over several weeks. The data of all six observers for preregistered  
287 Experiment 6 was collected before starting preregistered Experiment 7. The data of all six observers for  
288 preregistered Experiment 7 was collected before starting preregistered Experiment 8.

## 289 **Observer Recruitment and Exclusion**

290 The study recruited observers from North Carolina Agricultural and Technical State University and the  
291 local Greensboro community. The participants were compensated for their time. The observers underwent  
292 a screening process to meet criteria such as a normal visual acuity of 20/40 or better (with corrective  
293 eyewear if necessary) and normal color vision, which was assessed using pseudo-isochromatic plates  
294 (Ishihara, 1977). The preregistration documents outlined these exclusion criteria (see Methods:  
295 Preregistration).

296 We further conducted a practice session to identify observers who could reliably perform the  
297 psychophysical task. In the practice session, the observers' performed three blocks of the experiment for  
298 the no variation condition ( $\sigma^2 = 0.00$ ,  $\delta = 0.00$ ) and the threshold was calculated for these three blocks.  
299 If the mean threshold of the observer for the last two blocks in the practice session was larger than 0.030  
300 ( $\log T^2$ , -3.2), the observer was discontinued. The preregistration document specified this exclusion  
301 criteria (See Methods: Preregistration).

302 If the observers met these criteria, they were continued with the rest of the experiment.

303 For each observer, the practice session was performed at the beginning of each of the three experiments  
304 (Experiment 6, 7, 8), irrespective of whether the observer had participated in an earlier experiment.

## 305 **Observer Information**

306 Background reflectance variation (preregistered Experiment 6): A total of 25 observers participated in the  
307 practice sessions for background reflectance variation experiment (10 Female, 15 Male; age 19-34; mean  
308 age 22.9). Observers were given pseudo-names to deidentify their personal information from the data. Six  
309 of these observers (pseudo-names: *0003, bagel, committee, content, observer, and revival*) met the  
310 performance criterion set for screening (2 Female, 4 Male; age 19-28; mean age 23.33). Their visual  
311 acuity assessed using Snellen chart was 20/40 or better in both eyes and color vision assessed using  
312 Ishihara plates was normal. The visual acuities of the observers in the main experiment were: *0003, L =*  
313 *20/30, R = 20/20; bagel, L = 20/20, R = 20/20; committee, L = 20/25, R = 20/25; content, L = 20/20, R =*  
314 *20/20; observer, L = 20/25, R = 20/25; revival, L = 20/20, R = 20/20*. *Committee, content, and observer*  
315 *wore personal corrective eyewear both during vision testing and during the experiments. Observers 0003,*  
316 *bagel, and revival did not require or use corrective eyewear.*

317 Light source intensity variation (preregistered Experiment 7): A total of 15 observers participated in the  
318 practice sessions for light source intensity variation experiment (9 Female, 6 Male; age 19-33; mean age  
319 25). Six of these observers (pseudo-names: *0003, bagel, content, oven, primary, and revival*) met the  
320 performance criterion set for screening (3 Female, 3 Male; age 19-28; mean age 23.83). Their visual  
321 acuity assessed using Snellen chart was 20/40 or better in both eyes and color vision assessed using  
322 Ishihara plates was normal. The visual acuities of the observers in the main experiment were: *0003, L =*  
323 *20/30, R = 20/30; bagel, L = 20/20, R = 20/20; content, L = 20/20, R = 20/20; oven, L = 20/20, R =*  
324 *20/20; primary, L = 20/20, R = 20/20; revival, L = 20/20, R = 20/20*. Observer *content* and *primary* wore  
325 personal corrective eyewear both during vision testing and during the experiments. Observers *0003,*  
326 *bagel, oven, and revival* did not require or use corrective eyewear. Observer *oven* reported some  
327 difficulties during a few sessions of the experiment and their thresholds for two conditions did not fit the  
328 expected pattern. We removed their data from the analysis presented in this work. Their data and  
329 thresholds are provided as supplementary information (SI).

330     **Simultaneous variation (preregistered Experiment 8):** A total of 20 observers participated in the practice  
331 sessions for simultaneous variation experiment (9 Female, 11 Male; age 19-28; mean age 20.8). Six of  
332 these observers (pseudo-names: *0003, bagel, content, oven, manos, and revival*) were retained for the  
333 experiment (2 Female, 4 Male; age 19-28; mean age 23.33). Four observers (*0003, bagel, content, and*  
334 *oven*) met the screening criteria specified in the preregistration. Due to lack of observers who met the  
335 preregistration criteria, two observers (*manos, and revival*), whose thresholds were close to the  
336 preregistration criteria, were also retained for the experiment. Observer *revival* had participated in  
337 previous two experiments and had met the criteria both times. Observer *manos* showed improvement in  
338 thresholds with each block, with the threshold for the final block below 0.03. This was a deviation from  
339 the preregistration. Their visual acuity assessed using Snellen chart was 20/40 or better in both eyes and  
340 color vision assessed using Ishihara plates was normal. The visual acuities of the observers in the main  
341 experiment were: *0003, L = 20/30, R = 20/30; bagel, L = 20/20, R = 20/20; content, L = 20/20, R =*  
342 *20/20; oven, L = 20/20, R = 20/20; manos, L = 20/25, R = 20/25; revival, L = 20/20, R = 20/20*. Observer  
343 *content* wore personal corrective eyewear both during vision testing and during the experiments.  
344 Observers *0003, bagel, manos, oven, and revival* did not require or use corrective eyewear.

## 345     **Apparatus**

346     The experiments were performed in a dark room and the stimuli were presented on a color calibrated  
347 LCD monitor (27-in. NEC MultiSync EA271U; NEC Display Solutions). The pixel resolution of the  
348 monitor was selected as 1920 x 1080. Its refresh rate was 60Hz and each RGB channel was operated at 8-  
349 bit resolution. The experimental computer was an Apple Macintosh with an Intel Core i7 processor. The  
350 experimental programs were written in MATLAB (MathWorks; Natick, MA) and utilized Psychophysics  
351 Toolbox (<http://psychtoolbox.org>) and mgl (<http://justingardner.net/doku.php/mgl/overview>) libraries. A  
352 Logitech F310 gamepad controller was used to collect observers' response.

353     The distance between the observers' eyes and the monitor was set at 75cm. A forehead rest and chin cup  
354 (Headspot, UHCOTech, Houston, TX) were used to stabilize the observers' head position. The observers'  
355 eyes were centered both horizontally and vertically in relation to the display.

## 356     **Monitor Calibration**

357     The monitor was calibrated using a spectroradiometer (PhotoResearch PR655) as described in (Singh,  
358 Burge, & Brainard, 2022). The monitor was calibrated before starting each experiment. Once calibrated,  
359 the same settings were used till data for all observers for that experiment was collected. The monitor was  
360 then recalibrated for the next experiment. Data was collected in the sequence Experiment 6, Experiment  
361 7, and Experiment 8.

## 362     **Ethics Statement**

363     All experiments were approved by North Carolina Agricultural and Technical State University  
364 Institutional Review Board and were in accordance with the World Medical Association Declaration of  
365 Helsinki.

## 366     **Code and Data Availability**

367     The data for each experiment and observer is provided as supplementary information (SI). The SI is  
368 available at: <https://github.com/vijaysophie/SimultaneousVariationPaper>. The SI contains the proportion  
369 comparison chosen data as well as the thresholds for the 3 experimental blocks of each condition, for each  
370 experiment and observer. The MATLAB scripts to generate Figures 2, 6 – 12, supplementary Figures S1-

371 S7, and the scripts to obtain thresholds of the linear receptive field formulation of the model are also  
372 provided in the SI.

373 **Linear Receptive Field Model**

374 The thresholds of preregistered Experiment 6 were fit to the linear receptive field model developed in  
375 (Singh, Burge, & Brainard, 2022). This model consisted of a simple center surround receptive field ( $R$ ).  
376 The receptive field was square in shape to match the images in the psychophysics experiment. Its center  
377 was a circle of radius equal to the size and the location of the target object. The central region had a  
378 spatially uniform positive sensitivity of 1. The surround had a spatially uniform negative sensitivity of  $v_s$ .  
379 The receptive field response was computed as the dot product of the receptive field with the standard and  
380 the comparison images. A mean zero Gaussian noise was added to the response. The image with the  
381 higher noise added receptive field response was chosen to be lighter. The two parameters of the model,  
382 noise variance ( $\sigma_{ri}^2$ ) and surround sensitivity ( $v_s$ ), provided an estimate of the internal noise ( $\sigma_{ri}^2$ ) and the  
383 variance of the extrinsic properties ( $\sigma_{e0}^2$ ). The model related the thresholds ( $T$ ) in the experiments to the  
384 variance in the intrinsic noise ( $\sigma_{ri}^2$ ) of the observer and the extrinsic variance ( $\sigma_{e0}^2$ ) through the relation:

385 
$$T = \sqrt{\sigma_{ri}^2 + \sigma^2 \sigma_{e0}^2} \quad (1)$$

386 where  $\sigma^2$  is the covariance scalar (see (Singh, Burge, & Brainard, 2022) for details). The variance of the  
387 extrinsic properties ( $\sigma_{e0}^2$ ) resulting from the variation in the image can be computed as  $R^T \Sigma_{e0} R$ , where  
388  $\Sigma_{e0}$  is the covariance matrix of the variation in the images. We calculate the pixel-by-pixel covariance  
389 matrix of the image database for each condition and use the receptive field vector  $R$  to estimate the  
390 quantity  $R^T \Sigma_{e0} R$ .

391 Background reflectance variation: To estimate the variance of the intrinsic noise of the observer and  
392 extrinsic variation in the images, we chose the value of the Gaussian noise variance ( $\sigma_{ri,B}^2$ ) and the  
393 surround sensitivity  $v_{s,B}$  to minimize mean squared difference between the model and experimental  
394 thresholds measured at the six values of the covariance scalar.  $\sigma_{ri,B}^2$  provided the estimate of the intrinsic  
395 noise. The extrinsic noise ( $\sigma_{e0,B}^2$ ) was estimated by using the best fit surround sensitivity ( $v_{s,B}$ ) of the  
396 receptive field ( $R$ ) and the sample covariance matrix of the images ( $\Sigma_{e0}$ ) at  $\sigma^2=1$  in the relation  $R^T \Sigma_{e0} R$ .

397 Light source intensity variation: We fit a functional form similar to Eq. (1) to the thresholds of light  
398 source intensity variation experiment (Experiment 7) where we replaced covariance scalar  $\sigma^2$  by the  
399 range parameter  $\delta$ . We chose the value of the Gaussian noise variance ( $\sigma_{ri,L}^2$ ) and receptive field surround  
400 sensitivity ( $v_{s,L}$ ) to minimize the mean square difference between the observer and model thresholds  
401 measured at the seven values of the range parameter.  $\sigma_{ri,L}^2$  provided the estimate of the observer's intrinsic  
402 noise.

403 In natural viewing conditions, the intensity of the light source varies over several orders of magnitude  
404 (Singh, Cottaris, Heasly, Brainard, & Burge, 2018). This range of variation cannot be captured in the  
405 experiment due to the limitations of the monitor. To estimate the extrinsic noise, we used the best fit  
406 surround sensitivity ( $v_{s,L}$ ) and the sample covariance matrices to calculate the quantity  $R^T \Sigma_{e0} R$  as a  
407 function of the range parameter  $\delta$ . We fit the resulting values with an exponential function (see Figure  
408 S1). The extrinsic noise ( $\sigma_{e0,L}^2$ ) was chosen as the value of the exponential fit at  $\delta = 1$ . The parameter  
409 ( $\sigma_{e0,L}^2$ ) could be used to estimate the extrinsic noise for more naturalistic variations using the exponential  
410 fit.

411 **3 RESULTS**

412 **Human Lightness Discrimination Thresholds Increase with Background Reflectance Variation**

413 We measured lightness discrimination thresholds of human observers for two types of variation in the  
414 reflectance spectra of background objects in the scene: chromatic variation and achromatic variation. In  
415 chromatic variation, the reflectance spectra could take any shape and thus the background objects varied  
416 in their chromaticity and luminance. In achromatic variation, each spectrum had the same reflectance at  
417 all wavelengths, and thus the spectra varied only in their overall luminance and the objects were gray. The  
418 reflectance spectra were sampled from a statistical model of natural surface reflectance spectra database  
419 (See Methods: Reflectance and Illumination Spectra). The model approximated the database with a  
420 multivariate normal distribution whose covariance matrix was multiplied a covariance scalar ( $\sigma^2$ ) to  
421 control the amount of variation in the sampled spectra. We measured discrimination thresholds of six  
422 human observers at six values of the covariance scalar for chromatic variation and three values of  
423 covariance scalar for achromatic variation. For each of the nine conditions and for each observer,  
424 discrimination thresholds were measured three times in three separate blocks. The psychometric functions  
425 for these nine conditions are shown for one observer in Figure 6. The psychometric functions of all six  
426 observers are shown in Figure S3. We notice that as the covariance scalar increases, the slope of the  
427 psychometric functions decreases, corresponding to an increase in discrimination thresholds. The  
428 thresholds for chromatic and achromatic variation are comparable.

429 Figures 7 shows the change in discrimination thresholds as function of the variance in the reflectance of  
430 the background objects. Here we plot the mean log threshold squared (averaged across observers,  $N = 6$ )  
431 as a function of the log of the covariance scalar. The thresholds and standard error of the mean (SEM)  
432 from Figure 7 are listed in Table S1. We observe that the thresholds are nearly constant at small values of  
433 the covariance scalar. Once the value of the covariance scalar starts increasing, log threshold squared  
434 increases. Further, the thresholds are comparable for chromatic and achromatic variation. The p-values of  
435 the hypothesis that the mean thresholds for chromatic and achromatic variations are equal are 0.72, 0.57,  
436 and 0.16 for covariance scalar 0.03, 0.30, and 1.00 respectively, indicating that the differences in the  
437 mean thresholds are not statistically significant. Figure S3 shows the discrimination thresholds measured  
438 in preregistered Experiment 6 and previously reported thresholds in (Singh, Burge, & Brainard, 2022).  
439 The measured thresholds are consistent between the two experiments.

440 We fit the thresholds to the linear receptive field (LINRF) model (Eq. 1) developed in (Singh, Burge, &  
441 Brainard, 2022). The LINRF model provides the estimate of the variance of the internal noise of the  
442 observer as  $\sigma_{ri,B}^2 = 0.026$  and the variance of the extrinsic variability due to the reflectance of  
443 background objects as  $\sigma_{eo,B}^2 = 0.039$ . The equivalent noise level, the ratio of the external variance to  
444 intrinsic noise, is  $\sim 1.5$ , indicating that the variability in the representation of object lightness induced by  
445 the natural variability in the reflectance of background objects is close to the internal variability of that  
446 representation. If the ratio was equal to 1, then we would have concluded that the visual system has  
447 discounted the external variability. But the ratio is not significantly large compared to 1, this indicates that  
448 the visual system provides a significant level of lightness constancy.

449 **Human Lightness Discrimination Thresholds Increase with Light Source Intensity Variation**

450 We measured lightness discrimination thresholds of human observers as we varied the intensity of light  
451 sources in the scene. The shape of the spectrum of the light sources was fixed to be standard daylight  
452 spectrum D65. We normalized the spectrum by its mean over wavelengths. The intensity was varied by  
453 multiplying the normalized spectrum by a scalar sampled from a log-uniform distribution in the range [1-  
454  $\delta$ ,  $1 + \delta$ ]. The reflectance spectra of the background objects were fixed. We measured lightness  
455 discrimination thresholds for seven values of the range parameter  $\delta$  for five human observers. The

456 psychometric function of one of the observers for these seven conditions are shown in Figure 8. The  
457 psychometric functions of all six observers are shown in Figure S4. Figure 9 shows how the thresholds  
458 change as the amount of variation in the light source intensity increases. The data is averaged over five  
459 observers (also see Figure S5). Table S2 lists the mean thresholds and the SEM measured in this  
460 experiment. Similar to the trend for reflectance spectra variation, lightness discrimination thresholds  
461 remain constant for small values of the range parameter and then log threshold squared increases with  
462 increase in the range parameter. A fit of the mean squared threshold with the linear receptive field model  
463 gives the value of internal noise as  $\sigma_{ri,L}^2 = 0.028$ . This compares well with the internal noise obtained  
464 from the background reflectance spectra variation experiment ( $\sigma_{ri,B}^2 = 0.026$ ). The variance of the  
465 extrinsic variability estimated at range parameter  $\delta = 1.00$  is  $\sigma_{eo,L}^2 = 0.052$ . The equivalent noise level,  
466 the ratio of external variation to intrinsic noise is  $\sim 1.8$ . This indicates that the variation in the lightness  
467 representation induced by the variation in light source intensity is close to the internal variation of that  
468 representation at these levels. In natural conditions, where light source intensity varies over several order  
469 of magnitudes, the extrinsic noise can be estimated by generating images at the level of variation and  
470 using the LINRF model.

## 471 **Thresholds for Simultaneous Variation are Higher Than Individual Variations**

472 We measured lightness discrimination thresholds for simultaneous variation in the reflectance spectra of  
473 background objects and the intensity of the light sources in the scene. In this experiment, we studied six  
474 conditions: no variation, variation in the reflectance spectra of background objects with fixed spectrum of  
475 the light sources for achromatic and chromatic backgrounds, variation in intensity of light source with  
476 fixed background, and simultaneous variation in the intensity of light source and reflectance spectra of  
477 background object for chromatic and achromatic backgrounds. We measured lightness discrimination  
478 thresholds of six human observers for these six conditions. The psychometric function of one of the  
479 observers is shown in Figure 10. The psychometric functions of all six observers are shown in Figure S6.  
480 Figure 11 shows the mean log squared threshold of all six observers for these six conditions. Table S3  
481 lists the mean thresholds and SEM from Figure 11. The threshold for simultaneous variation of light  
482 source intensity and reflectance spectra of background objects is higher than the condition with individual  
483 variations in these properties. As observed earlier, the threshold for achromatic and chromatic conditions  
484 are comparable. The p-value of the hypothesis that the mean thresholds for chromatic and achromatic  
485 variations are equal is 0.19 for background variation condition and 0.44 for simultaneous variation  
486 condition, indicating that the differences in the mean thresholds are not statistically significant.

487 Figure 11 also shows the squared thresholds of the LINRF model for the six conditions. We used the  
488 intrinsic noise and the surround sensitivity ( $v_s$ ) parameters of the background reflectance variation  
489 experiment to estimate the threshold of the LINRF model for the no-variation condition, background  
490 spectra variation conditions, and the simultaneous variation conditions (Experiment 6, Figure 7). For the  
491 light intensity variation condition, we used the parameters of the light source intensity variation  
492 experiment (Experiment 7, Figure 9). See Figure S7 for the predictions of the LINRF model with same set  
493 of parameters for all six conditions.

494 We can use the linear receptive field model to compare the extrinsic variance of the simultaneous  
495 variation condition to the variance of the individual variations. According to the linear receptive model,  
496 the square of the threshold is proportional to the sum of the variance of observers' intrinsic noise and the  
497 extrinsic variation in the stimuli (Eq. 1). The squared threshold at the no variation condition is equal to the  
498 variance of the observers' intrinsic noise. In case of extrinsic variation, the increase in threshold square  
499 compared to the no variation condition equals the variance of the extrinsic variation. When there are more  
500 than one independent sources of extrinsic variation, the total variance of the simultaneous variation  
501 should be the sum of the variance of the individual variations. This predicts that the increase in threshold

502 square for simultaneous variation condition should be equal to the sum of the corresponding increase for  
503 the individual variation conditions.

504 Figure 12 shows the increase in mean squared threshold above the no variation condition. We compare  
505 the mean square thresholds of the simultaneous variation condition with the sum of the mean square  
506 thresholds of the individual conditions for chromatic and achromatic conditions. The increase in squared  
507 threshold of the simultaneous variation condition is comparable to the sum of the increase in squared  
508 threshold for the individual variations. The p-value of the hypothesis that the mean increase in squared  
509 thresholds for simultaneous variation is equal to sum of the mean increase in the squared thresholds of  
510 light intensity variation and background object reflectance variation are 0.86 and 0.80 for chromatic and  
511 achromatic conditions respectively. The variance of the extrinsic noise calculated for the background  
512 variation condition ( $\sigma^2 = 1.00, \delta = 0.00$ ) is 0.0015 and the light intensity variation condition ( $\sigma^2 =$   
513  $0.00, \delta = 0.30$ ) is 0.0017. As expected, the variance of the simultaneous variation condition ( $\sigma^2 = 1.00,$   
514  $\delta = 0.30$ ), which is 0.0033, is comparable to the sum of individual variances (0.0032).

## 515 4 DISCUSSION

516 The visual system is known to maintain a stable representation of object lightness despite variations in the  
517 proximal signal due to the scene. In this work we characterize the extent of such stability for variability in  
518 the spectra of background objects and light sources in a scene. We measured human observers' threshold  
519 of discriminating two objects based on their lightness as a function of amount of variation in these  
520 spectral properties. We observe that for low levels of variability, the thresholds first remained constant,  
521 showing that in this regime the performance was determined by observers' intrinsic noise. As the  
522 variability increased, the effect of extrinsic variation started dominating the performance and the  
523 discrimination thresholds increased. Using a model based on signal detection theory, we related the  
524 thresholds in the low variability regime to the internal noise of the observer. The model also related the  
525 increase in threshold to the amount of variability in the extrinsic property, thus providing a comparison of  
526 the variance in the extrinsic property to the intrinsic noise. The effect of both types of extrinsic variation,  
527 spectra of background objects and intensity of light sources, were comparable to the effect of intrinsic  
528 noise, showing that the visual system provides a good degree of constancy to these variations. Further, for  
529 simultaneous variation of these properties the effects added linearly, resulting in the variance of the  
530 simultaneous variation to be equal to the sum of the variance of the individual variations.

531 **Chromatic v/s Achromatic Variations:** Lightness discrimination thresholds of chromatic and  
532 achromatic variation in the reflectance spectra of background objects were statistically similar. The  
533 chromatic aspect of the variation does not seem to influence lightness discrimination, indicating that  
534 lightness and chromaticity are encoded independently. This hypothesis could be tested by measuring  
535 chromaticity discrimination thresholds under chromatic and achromatic variation of background objects.

536 **Visual system at threshold level:** For the spectral variabilities studied in this work, the variances in  
537 observers' representation of lightness due to extrinsic variations are within a factor of two compared to  
538 the variances in observers' intrinsic representation of lightness. If these variances were equal, one could  
539 conclude that the visual system has fully compensated for the extrinsic variation. As the extrinsic  
540 variances are larger than the variance of the intrinsic noise, the visual system has not fully compensated  
541 the external variabilities. But since these variances are within a factor of two, it shows that the visual  
542 system provides a large degree of stability in the perceptual representation of lightness and seems to work  
543 at near threshold levels.

544 **Rules of Combination:** The increase in squared threshold of simultaneous variation of reflectance  
545 spectra of background object and intensity of light sources from no variation condition were equal to the

546 sum of the increase in squared threshold of the individual variations. This could be accounted assuming  
547 that the sources of noise are independent, and their effects add linearly.

548 **5 ACKNOWLEDGEMENTS:** We thank Dr. David Brainard for his comments on the manuscript. This  
549 work was supported by National Science Foundation award BCS 2054900.

550  
551  
552

**Table S1: Thresholds for Background Variation Experiment (Preregistered Experiment 6):**  
 Mean threshold (averaged over blocks)  $\pm$  SEM of six human observers for nine background variation conditions studied in preregistered experiment 6.

Condition	Observer					
	0003	Bagel	Committee	Content	Observer	Revival
$\sigma^2 = 0.00$	0.0221 $\pm$ 0.0010	0.0185 $\pm$ 0.0018	0.0344 $\pm$ 0.0027	0.0223 $\pm$ 0.0012	0.0311 $\pm$ 0.0053	0.0251 $\pm$ 0.0023
$\sigma^2 = 0.01$	0.0215 $\pm$ 0.0009	0.0194 $\pm$ 0.0020	0.0386 $\pm$ 0.0103	0.0193 $\pm$ 0.0012	0.0263 $\pm$ 0.0059	0.0262 $\pm$ 0.0048
$\sigma^2 = 0.03$	0.0242 $\pm$ 0.0019	0.0261 $\pm$ 0.0020	0.0285 $\pm$ 0.0029	0.0246 $\pm$ 0.0046	0.0292 $\pm$ 0.0007	0.0282 $\pm$ 0.0016
$\sigma^2 = 0.03$ Achromatic	0.0255 $\pm$ 0.0019	0.0213 $\pm$ 0.0024	0.0343 $\pm$ 0.0055	0.0227 $\pm$ 0.0023	0.0267 $\pm$ 0.0040	0.0263 $\pm$ 0.0016
$\sigma^2 = 0.10$	0.0278 $\pm$ 0.0015	0.0238 $\pm$ 0.0010	0.0284 $\pm$ 0.0017	0.0278 $\pm$ 0.0035	0.0335 $\pm$ 0.0024	0.0281 $\pm$ 0.0013
$\sigma^2 = 0.30$	0.0348 $\pm$ 0.0025	0.0277 $\pm$ 0.0024	0.0344 $\pm$ 0.0020	0.0286 $\pm$ 0.0002	0.0277 $\pm$ 0.0019	0.0301 $\pm$ 0.0038
$\sigma^2 = 0.30$ Achromatic	0.0333 $\pm$ 0.0032	0.0284 $\pm$ 0.0028	0.0319 $\pm$ 0.0047	0.0308 $\pm$ 0.0015	0.0358 $\pm$ 0.0030	0.0287 $\pm$ 0.0022
$\sigma^2 = 1.00$	0.0416 $\pm$ 0.0072	0.0316 $\pm$ 0.0008	0.0379 $\pm$ 0.0024	0.0323 $\pm$ 0.0022	0.0405 $\pm$ 0.0042	0.0360 $\pm$ 0.0055
$\sigma^2 = 1.00$ Achromatic	0.0289 $\pm$ 0.0017	0.0310 $\pm$ 0.0015	0.0391 $\pm$ 0.0029	0.0384 $\pm$ 0.0058	0.0312 $\pm$ 0.0015	0.0322 $\pm$ 0.0009

553  
554  
555

**Table S2. Thresholds for Lightness Intensity Variation Experiment (Preregistered Experiment 7):**  
 Mean threshold (averaged over blocks)  $\pm$  SEM of six human observers measured for seven lightness intensity conditions studied in preregistered experiment 7. The thresholds of observer Oven were not used in Figure 9.

Condition	Observer					
	0003	Bagel	Content	Oven	Primary	Revival
$\delta = 0.00$	0.0217 $\pm$ 0.0012	0.0181 $\pm$ 0.0001	0.0208 $\pm$ 0.0014	0.0520 $\pm$ 0.0114	0.0329 $\pm$ 0.0061	0.0372 $\pm$ 0.0008
$\delta = 0.05$	0.0228 $\pm$ 0.0018	0.0229 $\pm$ 0.0018	0.0207 $\pm$ 0.0007	0.0580 $\pm$ 0.0064	0.0346 $\pm$ 0.0042	0.0364 $\pm$ 0.0013
$\delta = 0.10$	0.0275 $\pm$ 0.0024	0.0217 $\pm$ 0.0009	0.0242 $\pm$ 0.0040	0.0325 $\pm$ 0.0022	0.0343 $\pm$ 0.0013	0.0376 $\pm$ 0.0072
$\delta = 0.15$	0.0316 $\pm$ 0.0009	0.0238 $\pm$ 0.0011	0.0323 $\pm$ 0.0032	0.0333 $\pm$ 0.0019	0.0345 $\pm$ 0.0042	0.0326 $\pm$ 0.0002
$\delta = 0.20$	0.0447 $\pm$ 0.0100	0.0381 $\pm$ 0.0046	0.0276 $\pm$ 0.0016	0.0493 $\pm$ 0.0120	0.0423 $\pm$ 0.0050	0.0392 $\pm$ 0.0034
$\delta = 0.25$	0.0433 $\pm$ 0.0052	0.0393 $\pm$ 0.0062	0.0308 $\pm$ 0.0023	0.0461 $\pm$ 0.0060	0.0532 $\pm$ 0.0083	0.0387 $\pm$ 0.0025
$\delta = 0.30$	0.0404 $\pm$ 0.0018	0.0429 $\pm$ 0.0033	0.0347 $\pm$ 0.0014	0.0580 $\pm$ 0.0061	0.0465 $\pm$ 0.0047	0.0421 $\pm$ 0.0042

556

557  
558  
559

**Table S3. Thresholds for Simultaneous Variation Experiment (Preregistered Experiment 8):**  
 Mean threshold (averaged over blocks)  $\pm$  SEM of six human observers measured for six conditions studied in  
 preregistered experiment 8.

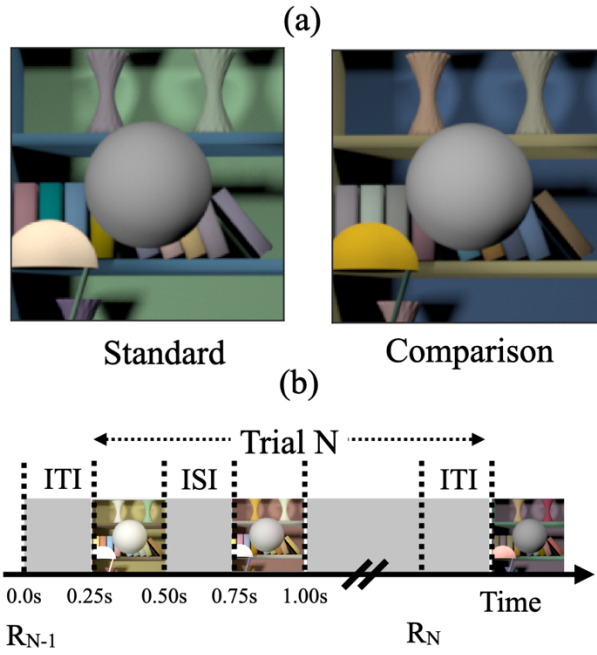
Condition	Observer					
	0003	Bagel	Content	Oven	Manos	Revival
No Variation	0.0261 $\pm$ 0.0022	0.0227 $\pm$ 0.0019	0.0246 $\pm$ 0.0004	0.0383 $\pm$ 0.0066	0.0258 $\pm$ 0.0036	0.0366 $\pm$ 0.0085
Background Variation Chromatic	0.0414 $\pm$ 0.0036	0.0340 $\pm$ 0.0058	0.0392 $\pm$ 0.0083	0.0498 $\pm$ 0.0050	0.0306 $\pm$ 0.0013	0.0383 $\pm$ 0.0033
Background Variation Achromatic	0.0394 $\pm$ 0.0027	0.0319 $\pm$ 0.0015	0.0427 $\pm$ 0.0074	0.0683 $\pm$ 0.0048	0.0435 $\pm$ 0.0071	0.0389 $\pm$ 0.0010
Light Intensity Variation	0.0464 $\pm$ 0.0027	0.0656 $\pm$ 0.0208	0.0412 $\pm$ 0.0021	0.0592 $\pm$ 0.0091	0.0464 $\pm$ 0.0046	0.0474 $\pm$ 0.0069
Simultaneous Variation Chromatic	0.0635 $\pm$ 0.0092	0.0536 $\pm$ 0.0014	0.0437 $\pm$ 0.0011	0.0639 $\pm$ 0.0106	0.0768 $\pm$ 0.0085	0.0528 $\pm$ 0.0037
Simultaneous Variation Achromatic	0.0648 $\pm$ 0.0103	0.0540 $\pm$ 0.0017	0.0478 $\pm$ 0.0049	0.0826 $\pm$ 0.0166	0.0749 $\pm$ 0.0082	0.0561 $\pm$ 0.0028

560

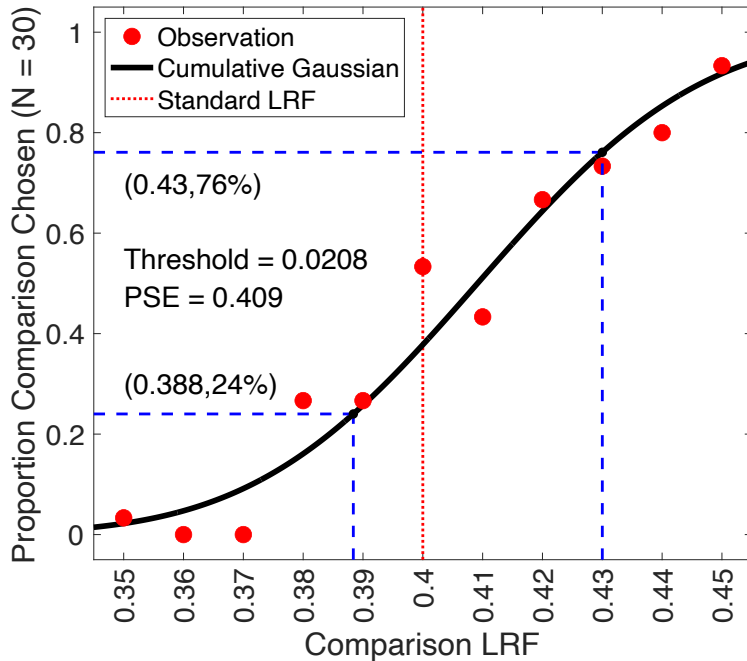
704 REFERENCES

- 705  
706 Adelson, E. (2000). Lightness Perception and Lightness Illusions. In M. S. Gazzaniga, *The New*  
707 *Cognitive Neurosciences* (pp. 339-351). Cambridge, MA: The MIT Press.  
708 American Society for Testing and Materials. (2017). *Standard test method for luminous*  
709 *reflectance factor of acoustical materials by use of integrating-sphere reflectometers.*  
710 Arend, L. E. (1993). How much does illuminant color affect unattributed colors? *Journal of the*  
711 *Optical Society of America*, 10(10), 2134-2147.  
712 Arend, L. E., & Goldstein, R. (1987). Simultaneous constancy, lightness, and brightness. *Journal*  
713 *of the Optical Society of America A*, 4(12), 2281-2285.  
714 Arend, L. E., & Goldstein, R. (1990). Lightness and brightness over spatial illumination  
715 gradients. *Journal of the Optical Society of America A*, 7(10), 1929-1936.  
716 Arend, L. E., & Spehar, B. (1993). Lightness, brightness, and brightness contrast: 1. Illuminance  
717 variation. *Perception & Psychophysics*, 54(4), 446-456.  
718 Arend, L. E., & Spehar, B. (1993). Lightness, brightness, and brightness contrast: 2. Reflectance  
719 variation. *Perception & Psychophysics*, 54(4), 457-468.  
720 Aston, S., Radonjic, A., Brainard, D. H., & Hurlbert, A. C. (2019). Illumination discrimination  
721 for chromatically biased illuminations: Implications for color constancy. *Journal of*  
722 *Vision*, 19(3), 1-15.  
723 Brainard, D. H. (1998). Color constancy in the nearly natural image. 2. Achromatic loci. *Journal*  
724 *of the Optical Society of America A*, 15(2), 307-325.  
725 Brainard, D. H., & Radonjic, A. (2004). Color constancy. *The visual neurosciences.*, 1, 948-961.  
726 Brainard, D. H., Brunt, W. A., & Speigle, J. M. (1997). Color constancy in the nearly natural  
727 image. Asymmetric matches. *Journal of the Optical Society of America A*, 14(9), 2091-  
728 2110.  
729 Bramwell, D. I., & Hurlbert, A. C. (1996). Measurements of colour constancy by using a forced-  
730 choice matching technique. *Perception*, 25(2), 229-241.  
731 Craven, B. J., & Foster, D. H. (1992). An operational approach to colour constancy. *Vision*  
732 *Research*, 32(7), 1359-1366.  
733 Delahunt, P. B., & Brainard, D. H. (2004). Does human color constancy incorporate the  
734 statistical regularity of natural daylight? *Journal of Vision*, 4(2), 57-81.  
735 Ennis, R., & Doerschner, K. (2019). Disentangling simultaneous changes of surface and  
736 illumination. *Vision Research*, 158, 173-188.  
737 Foster, D. H. (2003). Does colour constancy exist? *Trends in cognitive sciences*, 7(10), 439-443.  
738 Foster, D. H. (2011). Color constancy. *Vision Research*, 51(7), 674-700.  
739 Gilchrist, A. (2006). *Seeing black and white*. Oxford University Press.  
740 Hansen, T., Walter, S., & Gegenfurtner, K. R. (2007). Effects of spatial and temporal context on  
741 color categories and color constancy. *Journal of Vision*, 7(4), 1-15.  
742 Ishihara, S. (1977). *Tests for colour-blindness*. Tokyo: Kanehara Shuppon Company, Ltd.  
743 Jakob, W. (2010). Mitsuba Renderer.  
744 Kelly, K. L., Gibson, K. S., & Nickerson, D. (1943). Tristimulus specification of the Munsell  
745 book of color from spectrophotometric measurements. *Journal of the Optical Society of*  
746 *America*, 33(7), 355-376.  
747 Linhares, J. M., Pinto, P. D., & Nascimento, S. M. (2008). The number of discernible colors in  
748 natural scenes. *Journal of the Optical Society of America*, 25(12), 2918-2924.

- 749 Luo, M. R., Clarke, A. A., Rhodes, P. A., Schappo, A., Scrivener, S. A., & Tait, C. J. (1991).  
750        Quantifying colour appearance. Part I. LUTCHI colour appearance data. *Color Research*  
751        & Application, 16(3), 166-180.
- 752 Olkkonen, M., & Ekroll, V. (2016). Color constancy and contextual effects on color appearance.  
753        In J. Kremers, R. Baraas, & N. Marshall, *Human color vision, Springer Series in Vision*  
754        Research Vol. 5 (pp. 159-188). Springer, Cham.
- 755 Olkkonen, M., Hansen, T., & Gegenfurtner, K. R. (2009). Categorical color constancy for  
756        simulated surfaces. *Journal of Vision*, 9(12), 1-6.
- 757 Olkkonen, M., Witzel, C., Hansen, T., & Gegenfurtner, K. R. (2010). Categorical color  
758        constancy for real surfaces. *Journal of Vision*, 10(9), 1-16.
- 759 Patel, K. Y., Munasinghe, A. P., & Murray, R. F. (2018). Lightness matching and perceptual  
760        similarity. *Journal of vision*, 18(5), 1-13.
- 761 Pearce, B., Crichton, S., Mackiewicz, M., Finlayson, G. D., & Hurlbert, A. (2014). Chromatic  
762        illumination discrimination ability reveals that human colour constancy is optimised for  
763        blue daylight illuminations. *Plos One*, 9(2), e87989.
- 764 Reeves, A. J., Amano, K., & Foster, D. H. (2008). Color constancy: phenomenal or projective?  
765        *Perception & psychophysics*, 70(2), 219-228.
- 766 Rutherford, M. D., & Brainard, D. H. (2002). Lightness constancy: A direct test of the  
767        illumination-estimation hypothesis. *Psychological Science*, 13(2), 142-149.
- 768 Schultz, S., Doerschner, K., & Maloney, L. T. (2006). Color constancy and hue scaling. *Journal*  
769        *of Vision*, 6(10), 1-10.
- 770 Singh, V., Burge, J., & Brainard, D. H. (2022). Equivalent noise characterization of human  
771        lightness constancy. *Journal of Vision*, 22(5), 1-26.
- 772 Singh, V., Cottaris, N. P., Heasly, B. S., Brainard, D. H., & Burge, J. (2018). Computational  
773        luminance constancy from naturalistic images. *Journal of Vision*, 18(3), 1-19.
- 774 Smithson, H., & Zaidi, Q. (2004). Colour constancy in context: Roles for local adaptation and  
775        levels of reference. *Journal of Vision*, 4(9), 1-3.
- 776 Speigle, J. M., & Brainard, D. H. (1996). Is color constancy task independent? *Color and*  
777        *Imaging Conference*. 1, pp. 167-172. Society for Imaging Science and Technology.
- 778 Troost, J. M., & De Weert, C. M. (1991). Naming versus matching in color constancy.  
779        *Perception & psychophysics*, 50, 591-602.
- 780 Uchikawa, K., Uchikawa, H., & Boynton, R. M. (1989). Partial color constancy of isolated  
781        surface colors examined by a color-naming method. *Perception*, 18(1), 83-91.
- 782 Vrhel, M. J., Gershon, R., & Iwan, L. S. (1994). Measurement and analysis of object reflectance  
783        spectra. *Color Research & Application*, 19(1), 4-9.
- 784



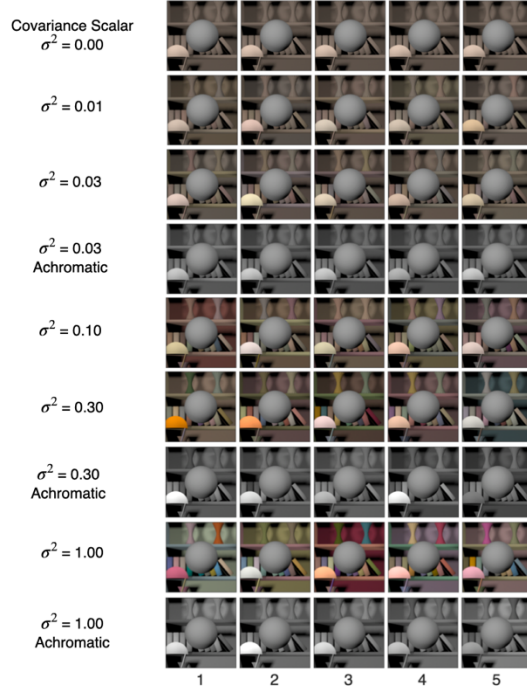
1  
2 **Figure 1: (a) Psychophysical task.** (Adapted from Figure 1 in Singh, Burge, & Brainard, 2022) The  
3 psychophysical task involved comparing two images, a standard image and a comparison image, on each  
4 trial and selecting the image with the lighter target object. The target object was an achromatic sphere at  
5 the center of the image. The images were generated computationally by graphically rendering models of  
6 3D scenes. They were displayed on a color calibrated monitor. This panel shows examples of standard  
7 and comparison images. The reflectance spectrum of the target object was spectrally flat, and the target  
8 object appeared gray. The reflectance of the target object in the standard image was held fixed and it  
9 changed for the comparison image. In this panel, the target object in the comparison image is lighter. We  
10 measured the fraction of times the observers chose the target object in the comparison image to be lighter  
11 as a function of the lightness of the target object in the comparison image. Fraction comparison chosen  
12 data was used to determine lightness discrimination threshold (Figure 2). We studied how the lightness  
13 discrimination thresholds changed as the trial-to-trial variability in the reflectance spectra of the  
14 background objects and the intensity of the light sources increased. **(b) Trial sequence:**  $R_{N-1}$  indicates the  
15 recording of the observer's response for the  $(N-1)^{th}$  trial. The  $N^{th}$  trial begins 250ms after the completion  
16 of the  $(N-1)^{th}$  trial (Inter Trial Interval, ITI = 250ms). In the  $N^{th}$  trial, the standard and comparison images  
17 are presented for 250ms each with a 250ms inter stimulus interval (ISI) in between the two images. The  
18 order of the standard and comparison images is chosen in pseudorandom order. The observer records their  
19 choice by pressing a button on a gamepad after both images have been presented and removed from the  
20 screen. The observers could take as long as they wish before making their choice. The recording of their  
21 choice is indicated by  $R_N$  in the panel. The next trial begins 250ms after the choice has been recorded.



1

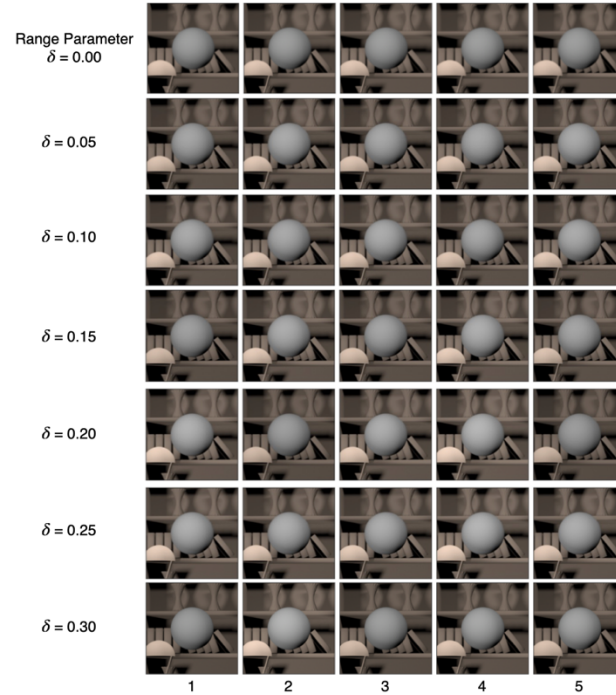
2 **Figure 2: Psychometric function:** We measured the proportion of times the observers selected the target  
 3 in the comparison image to be lighter as function of the LRF (lightness reflectance factor) of the target  
 4 object. We collected 30 responses for each of the 11 equally spaced values of the comparison image target  
 5 object LRF, ranging from 0.35 to 0.45. The target object in the standard image had an LRF of 0.40. The  
 6 LRF of the target object in the comparison image was selected in a pseudorandom order. To analyze the  
 7 data, we used maximum likelihood methods to fit a cumulative normal function to the proportion  
 8 comparison chosen data. We imposed constraints on the guess rate and lapse rate, requiring them to be  
 9 equal and within the range of 0 to 0.05. The threshold was determined as the difference between the LRF  
 10 values corresponding to a proportion comparison chosen of 0.76 and 0.50, obtained from the cumulative  
 11 normal fit. The figure presented here illustrates the data for observer 0003 in the second block of the  
 12 background reflectance variation experiment (previously registered as Experiment 6) for the no variation  
 13 ( $\sigma^2 = 0.00, \delta = 0.00$ ) condition. The discrimination threshold was measured to be 0.0208. The point of  
 14 subjective equality (PSE), which corresponds to a proportion of 0.5 in the comparison task, was found to  
 15 be 0.409. The lapse rate for this particular fit was determined to be 0.00.  
 16

1



2 **Figure 3: Background object reflectance variation:** We studied two types of variations in the  
 3 reflectance spectra of background objects in the scene: chromatic variation and achromatic variation. In  
 4 chromatic variation, the reflectance spectra could take any shape, and the objects varied in their  
 5 luminance and chromaticity. In achromatic variation, the reflectance spectra were spectrally flat, and the  
 6 objects appeared gray and varied only in their luminance. The spectra were chosen from a multivariate  
 7 normal distribution that modeled the statistics of natural reflectance spectra. The covariance matrix of the  
 8 multivariate normal distribution was multiplied by a scalar to control the variance in the samples. We  
 9 generated images at six logarithmically spaced values of the covariance scalar for chromatic variation and  
 10 at three values of the covariance scalar for achromatic variations. The figure shows five typical images for  
 11 each of these nine conditions. For each condition we generated 1100 images, 100 images at 11 linearly  
 12 spaced value of target object LRF in the range [0.35, 0.45]. The target object in each image in the figure is  
 13 at LRF = 0.4.

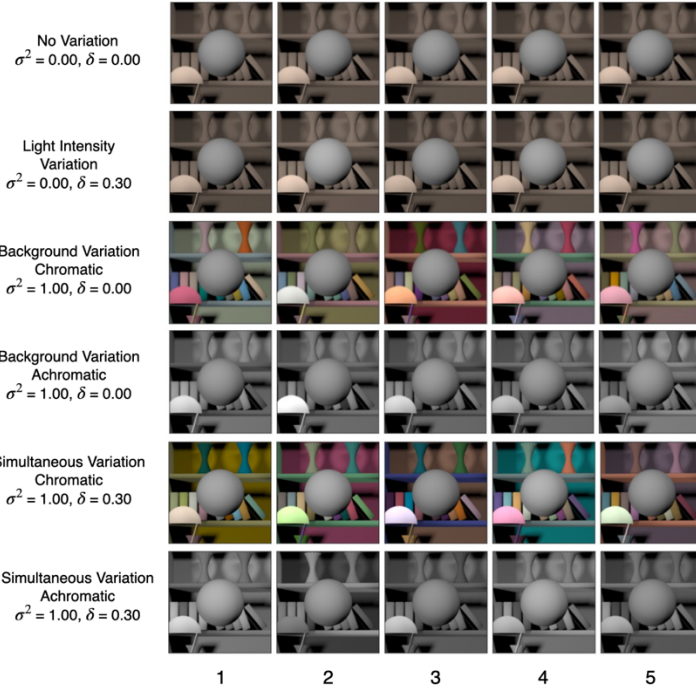
1



2 **Figure 4: Light intensity variation:** The shape of the power spectrum of the light sources in the scene  
3 was chosen to be CIE reference illuminant D65. The intensity of the power spectrum was varied by  
4 multiplying the normalized D65 spectrum with a scalar sampled from a log uniform distribution in the  
5 range  $[1 - \delta, 1 + \delta]$ . The amount of variation was controlled by changing the value of the range parameter  
6  $\delta$ . We generated images at seven linearly spaced values of the range parameter in the range  $[0.00, 0.30]$ .  
7 For each value of the range parameter, we generated 1100 images, 100 images at each value of the target  
8 object LRF in the range  $[0.35, 0.45]$ . The figure shows five sample images at each of the seven values of  
9 the range parameter. The target object in each image in the figure has the same LRF of 0.40.

1

2 **Figure 5: Simultaneous variation:** This figure shows five sample images for the six conditions studied  
 3 in preregistered Experiment 8. We generated 1100 images for each of these conditions, 100 images at  
 4 each value of the target object LRF in the range [0.35, 0.45].



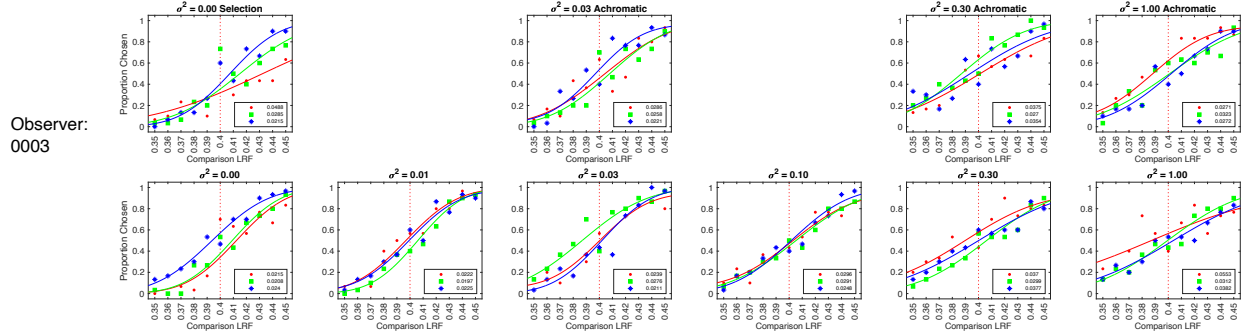
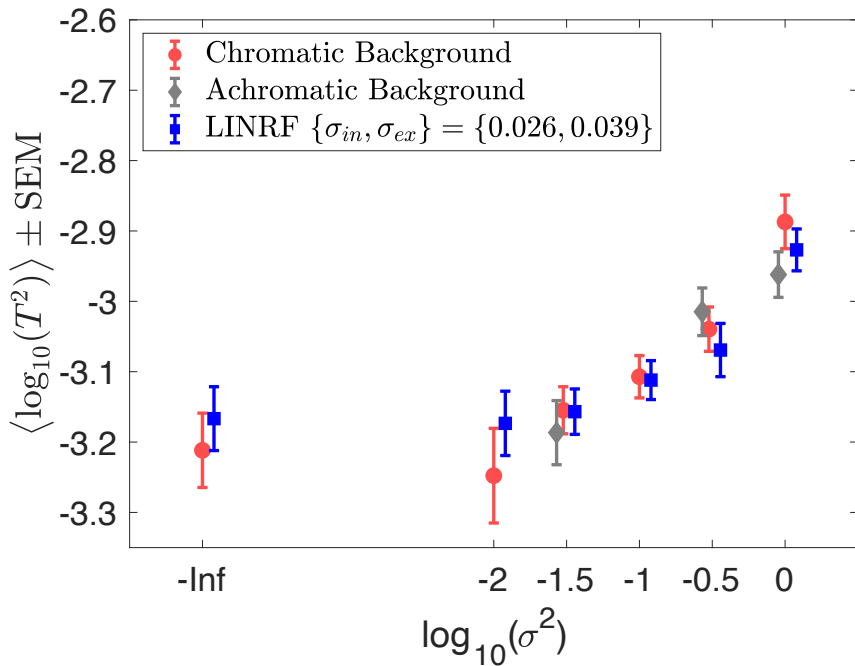


**Figure 6: Psychometric functions for observer 0003 for background reflectance variation**

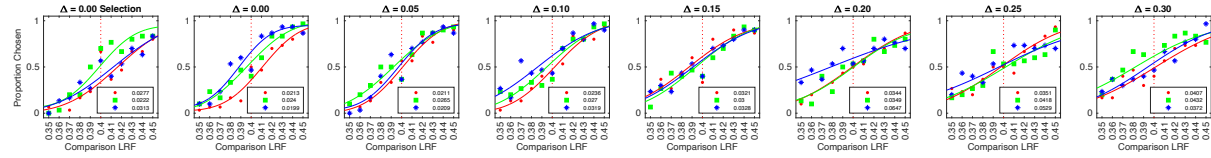
**experiment:** We measured the proportion comparison chosen data for the nine conditions separately in three blocks for each observer. The figure shows the psychometric function for observer 0003. The psychometric functions for all six observers are shown in Figure S2. A cumulative normal function was fit to the data from each block to determine the discrimination threshold (see Figure 2). The legend provides the estimated lightness discrimination threshold for each block, obtained from the cumulative fit. The first panel in the top row shows the data and thresholds for the selection session. The selection session was a practice session in which the thresholds for the no variation condition was measured three times. An observer was selected for the experiment only if the average of their last two discrimination threshold measurements in the selection session was less than 0.30. The last three panels in the top row show the data for the three achromatic conditions. The bottom row shows the data for the chromatic variation conditions.



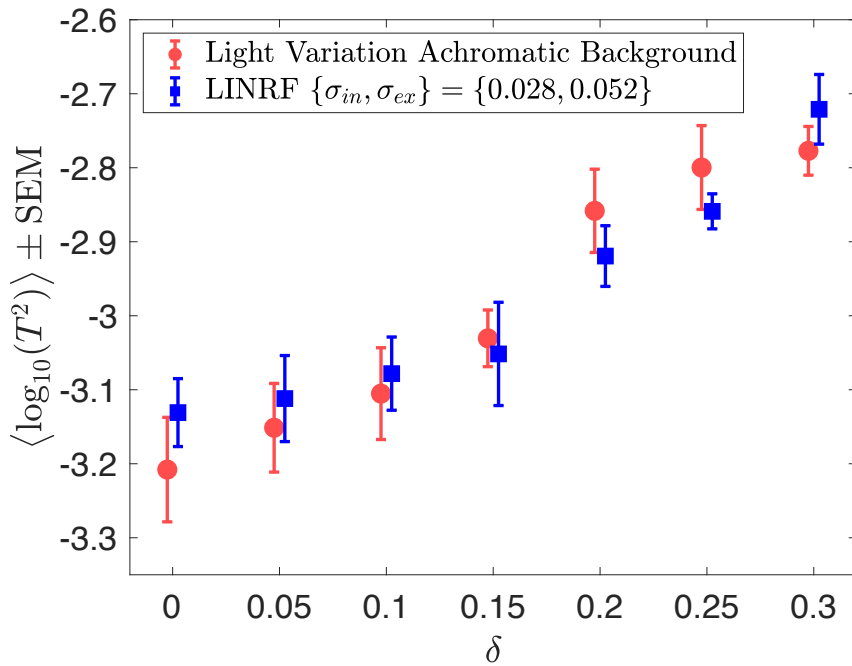
1

2 **Figure 7: Background variation increases lightness discrimination thresholds.** Mean (N = 6) log  
 3 squared threshold vs log covariance scalar from human psychophysics for chromatic (red circles) and  
 4 achromatic conditions (gray diamonds). The error bars represent +/- 1 SEM taken between observers. The  
 5 threshold of the linear receptive field (LINRF) model was estimated by simulation for the six values of  
 6 the covariance scalar (blue squares). The blue error bars show +/- 1 standard deviation estimated over 10  
 7 independent simulations. The legend shows the parameters of the linear receptive field (LINRF) model  
 8 fit. The data has been jittered for ease of viewing. A comparison of the thresholds with the previously  
 9 published data in Singh, Burge, Brainard 2022 is shown in Figure S3.

1



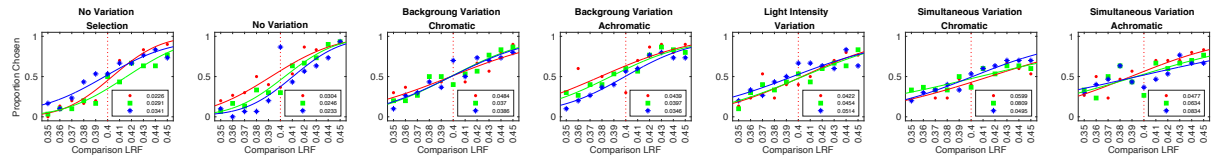
2 **Figure 8: Psychometric functions for observer 0003 for light intensity variation experiment:** Same  
3 as Figure 6, but for the light intensity variation experiment. The figure shows the proportion comparison  
4 chosen data for the selection session and the seven condition for observer 0003. The psychometric  
5 functions for all observers are shown in Figure S4.



1

2 **Figure 9: Light source intensity variation increases lightness discrimination threshold.** Mean (N = 5)  
3 log squared threshold vs range parameter from human psychophysics for the seven light source intensity  
4 variation conditions (red circles). The error bars represent +/- 1 SEM taken between observers. The  
5 threshold of the linear receptive field (LINRF) model was estimated by simulation for the seven values of  
6 the range parameters (blue squares). The blue error bars show +/- 1 standard deviation estimated over 10  
7 independent simulations. The legend shows the parameters of the LINRF model fit. The data has been  
8 jittered for ease of viewing. The data for all six observers is shown in Figure S5.

1



2 **Figure 10: Psychometric functions for observer 0003 for simultaneous variation experiment:** Same  
3 as Figure 6 and 8, but for simultaneous variation experiment. The figure shows the proportion comparison  
4 chosen data for the selection session and the six condition for observer 0003. The data for all observers  
5 are shown in Figure S6.

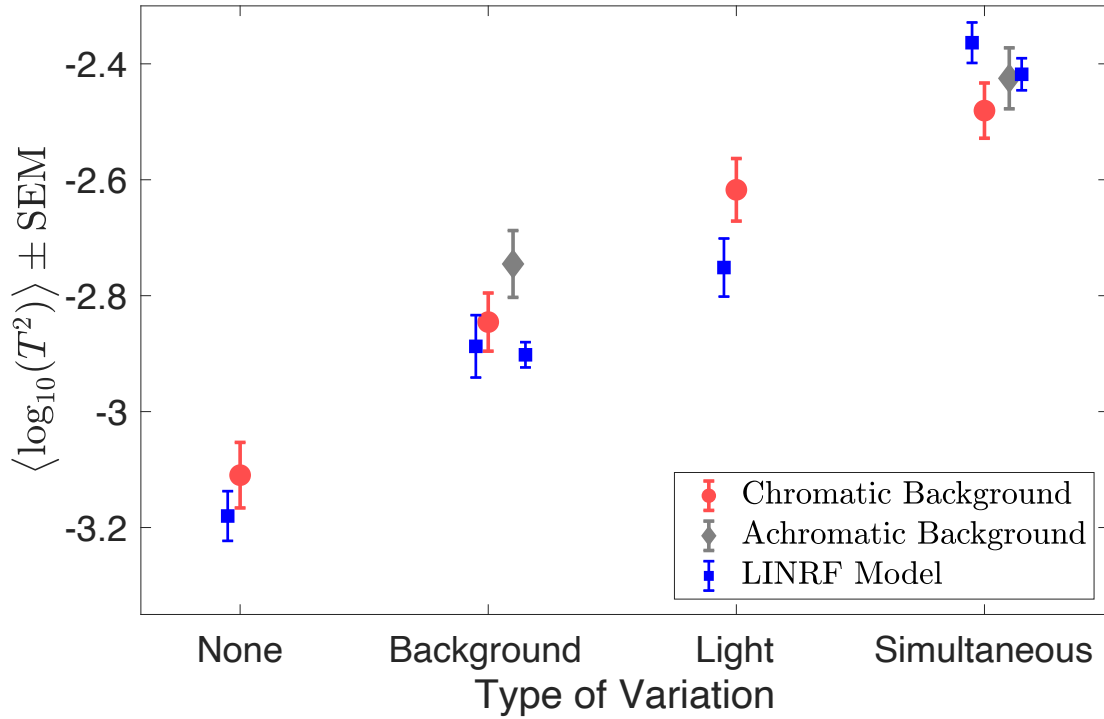
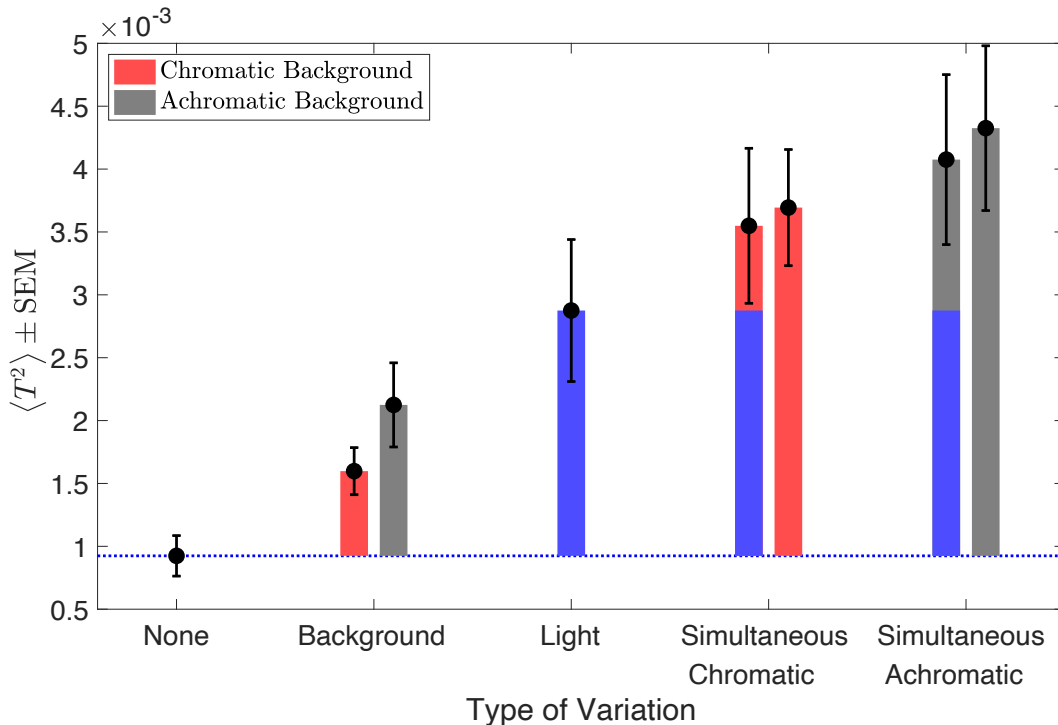
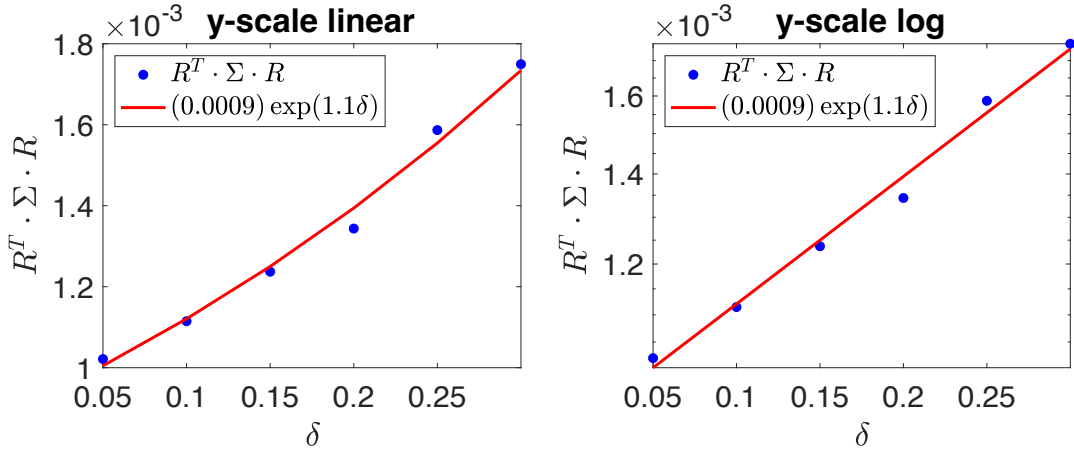


**Figure 11: Discrimination thresholds for simultaneous variation of two sources are higher than individual discrimination thresholds.** Mean ( $N = 6$ ) log squared threshold for the six conditions in simultaneous variation experiment. The error bars represent  $\pm 1$  SEM taken between observers. The data for chromatic (red circles) and achromatic (gray diamonds) conditions have been plotted next to each other for visual comparison. The thresholds of the linear receptive field (LINRF) model (blue squares) were estimated using the parameters of the background variation condition (Figure 7) for the None, Background variation and Simultaneous variation conditions and using the parameters of the light intensity variation condition (Figure 9) for the Light condition. The blue error bars show  $\pm 1$  standard deviation estimated over 10 independent simulations. See Figure S7 for LINRF model thresholds with the same set of parameters for all conditions.



1

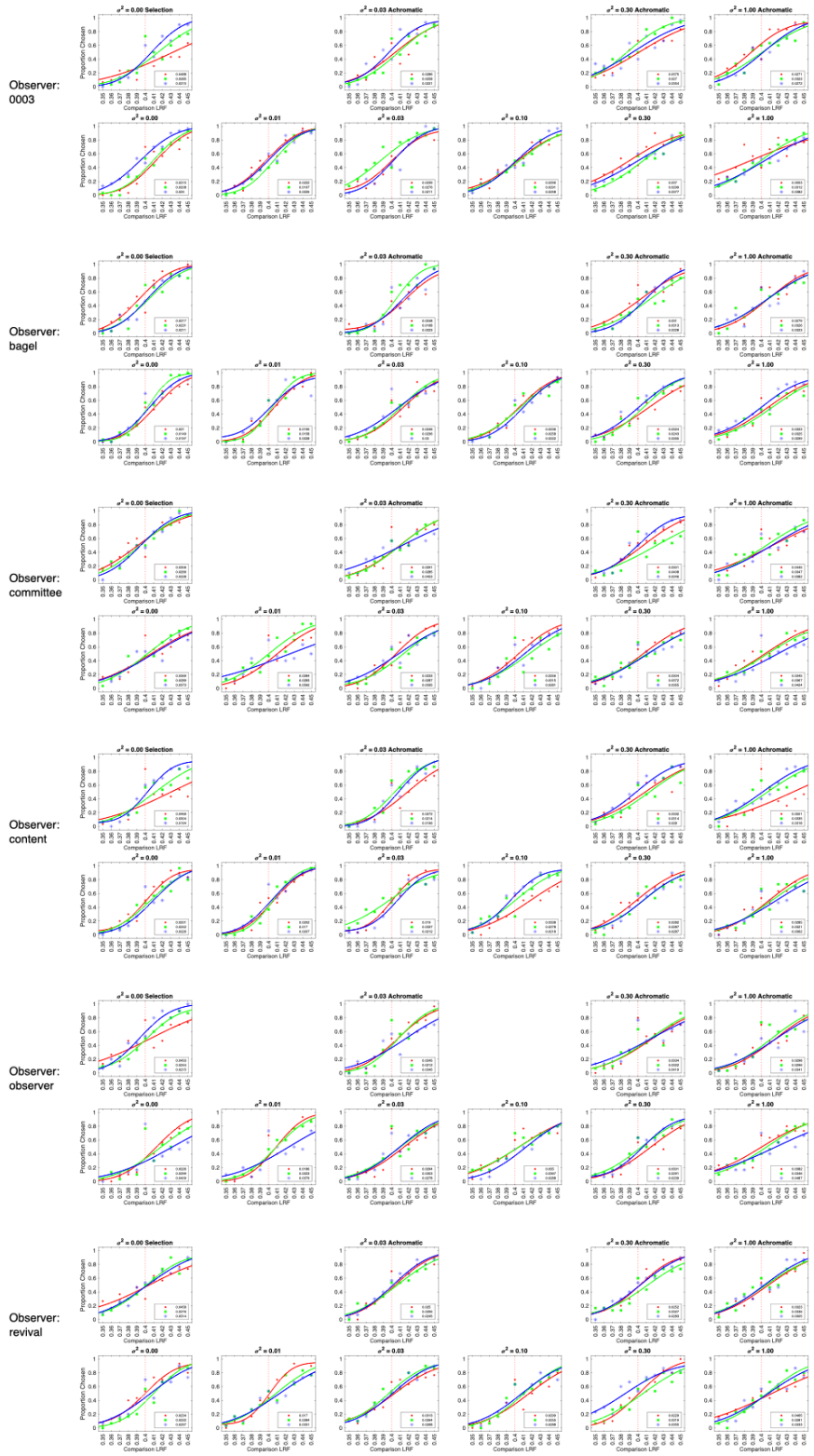
2 **Figure 12: Extrinsic noise of independent variations add linearly for simultaneous variation:** Mean  
3 squared thresholds ( $N=6$ ) for the six conditions in simultaneous variation experiment (black circles). The  
4 black error bars represent  $\pm 1$  SEM taken between observers. The bars (red, gray, blue) represent the  
5 increase in squared thresholds compared to the no variation condition (blue dotted line). For the  
6 simultaneous variation conditions, the bars on the right (bars with one color, red or gray) represent the  
7 increase in measured squared threshold for the simultaneous variation conditions and the bars on the left  
8 (stacked bars of two different colors) represent the increase in the sum of the squared threshold of the  
9 light intensity variation (blue bar) and the corresponding background variation conditions (red or gray).

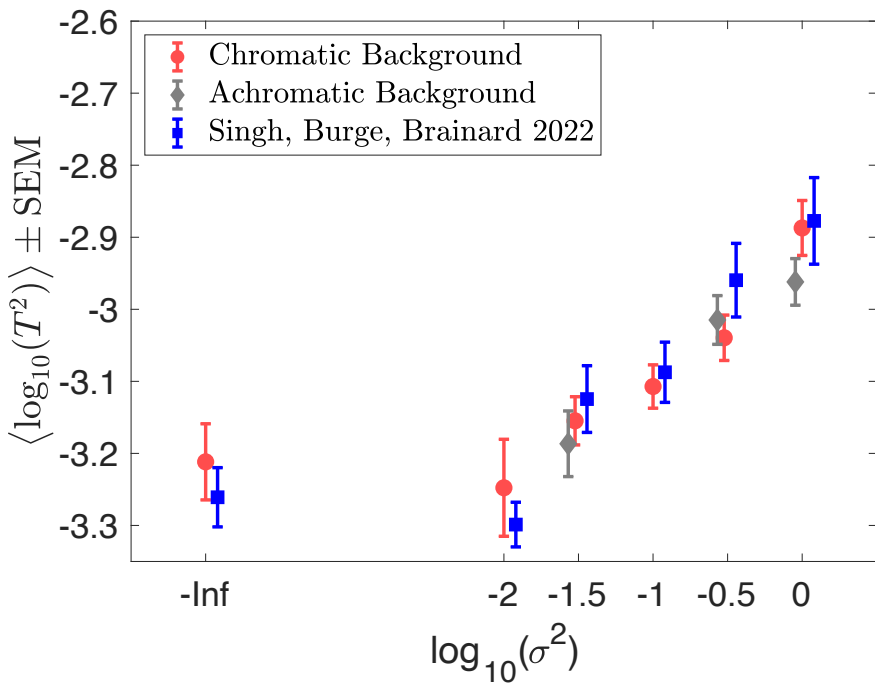


1

2 **Figure S1: Estimation of extrinsic noise for light intensity variation:** Plot of the variance ( $R^T \Sigma R$ ) as a  
3 function of the range parameter  $\delta$  on a linear (left panel) and logarithmic (right panel) scale. We fit the  
4 function with an exponential of the form  $A * \exp(B \cdot \delta)$ . The variance in the extrinsic noise is estimated  
5 as the value of the fit at  $\delta = 1$ .

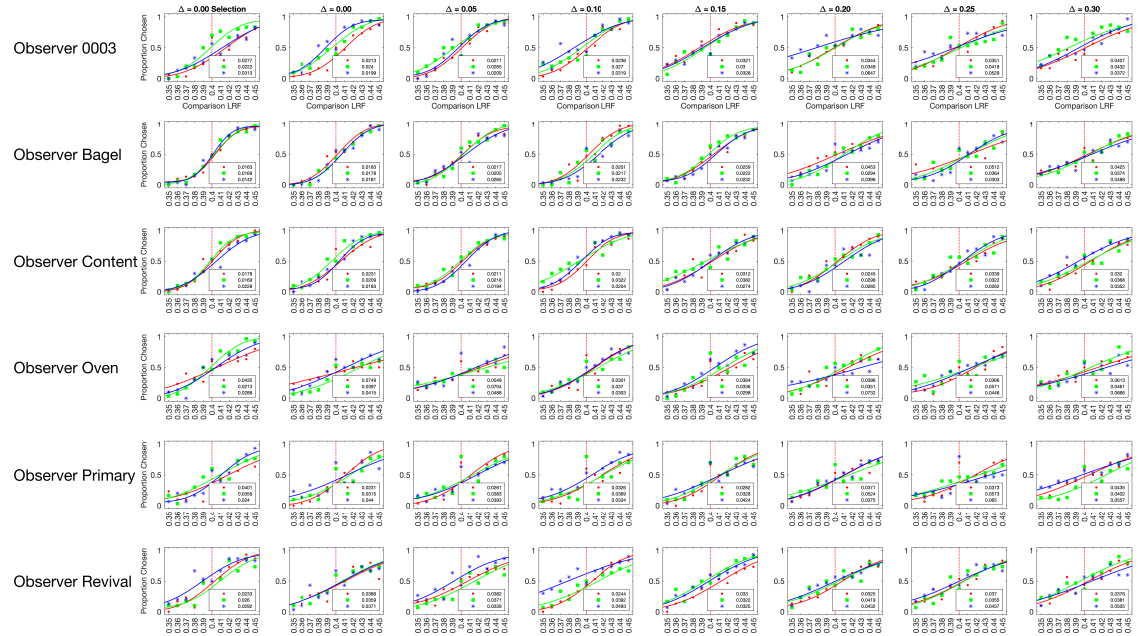
2 **Figure S2: Psychometric functions for all observers for background variation experiment.** Same as  
3 Figure 6, for all observers retained in background variation experiment.





1

2 **Figure S3: Comparison with Singh, Burge, Brainard 2022.** Lightness discrimination thresholds for  
3 background variation condition measured in preregistered Experiment 6 and previously reported data  
4 from Singh, Burge, Brainard 2022. Preregistered Experiment 6 had both chromatic and achromatic  
5 conditions, while the previous experiment (Singh, Burge, Brainard 2022) only had chromatic condition.  
6 Singh, Burge, Brainard 2022 made three threshold measurements for each condition for 4 naïve  
7 observers.

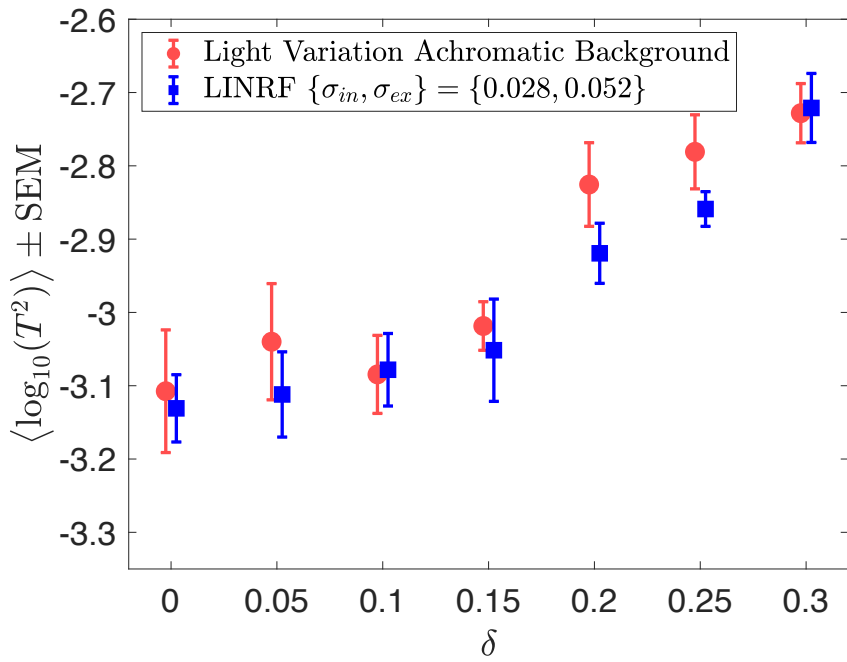


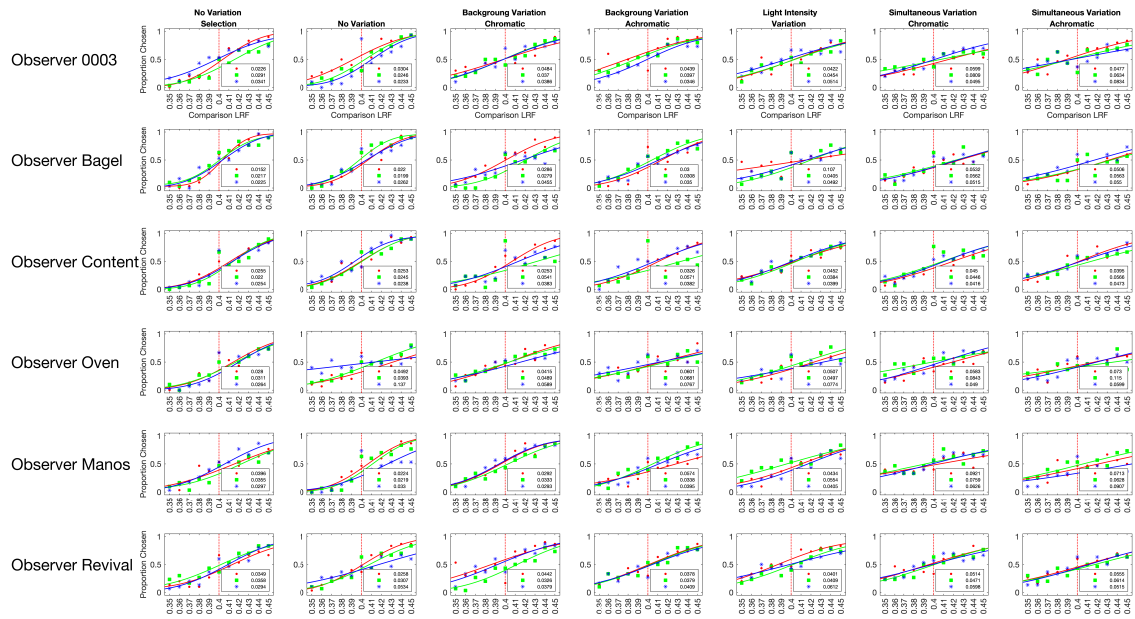
1

2 **Figure S4: Psychometric functions for all observers for light intensity variation experiment.** Same  
3 as Figure 8, for all observers retained in light intensity variation experiment.

1

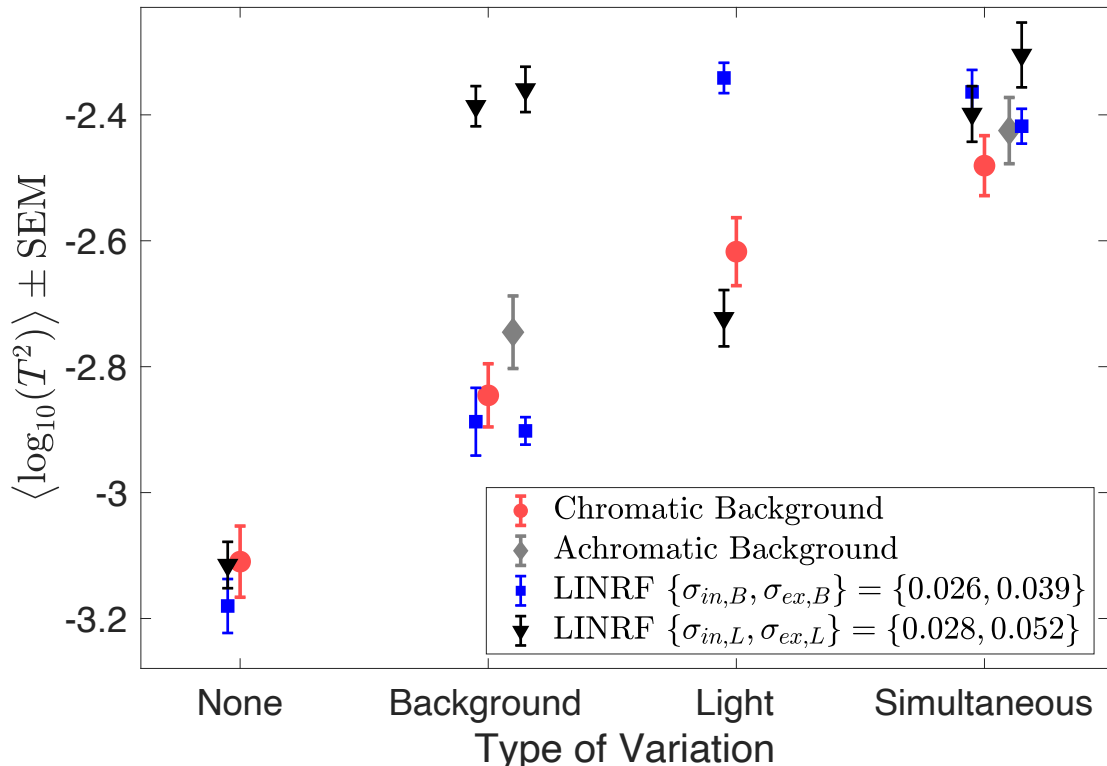
2 **Figure S5:** Same as Figure 9, for all six observers retained in light intensity variation experiment. The  
3 parameters for the LINRF model are the same as in Figure 9.





1

2 **Figure S6: Psychometric functions for all observers for simultaneous variation experiment.** Same as  
3 Figure 10, for all observers retained in simultaneous variation experiment.



1  
 2 **Figure S7:** Same as Figure 11, but the thresholds of the linear receptive field (LINRF) model were  
 3 estimated using the same set of parameters for all six conditions studied in Experiment 8. Blue square  
 4 markers show log squared thresholds estimated using the parameters of the background variation  
 5 condition (Experiment 6, Figure 7). Black triangular markers show log squared thresholds estimated using  
 6 the parameters of the light intensity variation condition (Experiment 7, Figure 9). The black and blue error  
 7 bars show +/- 1 standard deviation estimated over 10 independent simulations. The parameters of the  
 8 background variation condition (Experiment 6, blue squares) predict the thresholds of the no variation  
 9 condition, the background variation condition, and the simultaneous variation condition quite well, but  
 10 fail to predict the threshold of the light source intensity variation condition. Similarly, the parameters of  
 11 the light source intensity variation condition (Experiment 7, black triangles) predict the thresholds of the  
 12 no variation condition, the light source intensity variation condition, and the simultaneous variation  
 13 condition quite well, but fail to predict the threshold of the background variation condition. This could  
 14 possibly be because observers in the three experiments were different. Future work would aim at studying  
 15 these conditions using the same set of observers.